

Holographic entanglement entropy in $T\bar{T}$ -deformed AdS_3

Miao He^{a,b}, Yuan Sun^c

^a*School of Physics, Southeast University, Nanjing 211189, China*

^b*Shing-Tung Yau Center, Southeast University, Nanjing 210096, China*

^c*School of Physics and Electronics, Central South University, Changsha 418003, China*

E-mail: hemiao@seu.edu.cn, sunyuan@jlu.edu.cn

Abstract

In this work, we study the holographic entanglement entropy in AdS_3 gravity with the certain mixed boundary condition, which turns out to correspond to $T\bar{T}$ -deformed 2D CFTs. By employing the Chern-Simons formalism and Wilson line technique, the holographic entanglement entropy in $T\bar{T}$ -deformed BTZ black hole is obtained. We also get the same formula by calculating the RT surface. The holographic entanglement entropy agrees with the perturbation result derived from both $T\bar{T}$ -deformed CFTs and cutoff AdS_3 . Moreover, our result shows that the deformed entanglement entropy for large deformation parameter behaves like the entanglement entropy of CFT at zero temperature. We also consider the entanglement entropy of two intervals and study the effect of $T\bar{T}$ deformation on phase transition.

Contents

1	Introduction	1
2	Wilson lines and entanglement entropy in AdS₃	3
2.1	Wilson lines in AdS ₃ gravity	4
2.2	Equivalence to the geodesic equation	6
2.3	Holographic entanglement entropy	7
2.3.1	Poincaré AdS ₃	8
2.3.2	BTZ black hole	9
2.4	Loops and thermal entropy	11
3	Holographic entanglement entropy in $T\bar{T}$- deformed AdS₃	12
3.1	$T\bar{T}$ deformed AdS ₃ geometry	12
3.2	$T\bar{T}$ -deformed holographic entanglement entropy	14
3.3	Thermal entropy	19
3.4	Two intervals entanglement entropy	20
4	Geodesic line method	23
5	Conclusion and discussion	25
A	Conventions	26
B	Wilson line defects	27

1 Introduction

The AdS/CFT correspondence gives a geometric interpretation to the conformal field theory. This correspondence allows us to study quantum gravity from the conformal field theory, and it achieves great success in 3D quantum gravity. It is significant to generalize the AdS/CFT correspondence by deforming the conformal field theory and investigating its geometric interpretation. One of the deformed theories called $T\bar{T}$ deformation was proposed and its holographic descriptions were also explored [1–4]. It is interesting to establish the holographic dictionary under $T\bar{T}$ deformation. The holographic technique also provides us with a gravitational method to study the $T\bar{T}$ deformed CFT.

The $T\bar{T}$ deformation is defined through the $T\bar{T}$ flow equation

$$\frac{\partial S_{T\bar{T}}}{\partial \mu} = \int d^2x \mathcal{O}_{T\bar{T}}, \quad \mathcal{O}_{T\bar{T}} \equiv T^{ij}T_{ij} + T^2,$$

where T_{ij} is the stress tensor of the deformed theory. This flow equation generates a family of integrable field theory if the original theory is integrable [1, 2]. The factorization of $T\bar{T}$ operator leads to the Burgers equation for the deformed spectrum [5], so that the spectrum of the deformed theory can be exactly solved. The partition function of the deformed theory can be obtained from various methods, the result turns out that the deformed partition function satisfies a differential equation or an integral transformation of the original one [6–8]. The deformed partition function is still modular invariant [9]. According to the $T\bar{T}$ flow equation, the Lagrangian form and Hamiltonian form were also studied [10, 11]. There are also some evidences shown that the $T\bar{T}$ deformed theory is a non-local theory [12–16]. In this irrelevant deformation, it is difficult to study the local properties, such as the correlation function and entanglement entropy. These observables play the important role in the quantum field theory. By using the perturbative method, the correlation functions and entanglement entropy have also been obtained [21–31]. Some non-perturbative results about the correlation function and entanglement were explored in [17–20]. However, there is still an open question to calculate the correlation function and entanglement entropy in $T\bar{T}$ deformed theory. For a pedagogical review see [32].

According to the AdS/CFT correspondence, the deformed theory can be investigated by using the gravitational approach. There are two points of view to understand the $T\bar{T}$ deformed CFTs from gravity. The one is the $T\bar{T}$ deformed CFTs dual to the AdS₃ with a finite radial cutoff [3, 4]. In this situation, the quasi-local energy of the cutoff region matches the spectrum of the deformed theory. The $T\bar{T}$ flow equation coincides with the Hamilton-Jacobi equation governing the radial evolution of the classical gravity action in AdS₃. Many holographic features of the $T\bar{T}$ deformed CFT have been explored based on the cutoff perspective [33–42]. The other holographic perspective to understand the $T\bar{T}$ deformation is the AdS₃ gravity with certain mixed boundary condition [43]. The boundary condition was derived through the flow equation and variational principle. It turned out that the solution of the metric flow equation related to the higher order Fefferman-Graham expansion, which leads to the mixed boundary condition. For the positive deformation parameter, the mixed boundary condition coincides with the induced metric on the finite radial cutoff. The AdS₃ solutions that satisfy the mixed boundary condition were also constructed from AdS₃ with Brown-Henneaux boundary condition [44] through a field-dependent coordinate transformation [43]. The dynamic coordinate transformation approach to $T\bar{T}$ was also found in field theoretic results [45, 46]. The deformed spectrum can also be obtained from the deformed AdS₃. Moreover, the mixed boundary condition allows boundary graviton degree of freedom, which turns out to be a $T\bar{T}$ deformed theory [47–50]. It also provides us with another approach to studying the $T\bar{T}$ deformation including the holographic entanglement entropy.

In this paper, we would like to investigate the entanglement entropy in $T\bar{T}$ deformed CFT from holography. For the cutoff perspective, the holographic entanglement was obtained by calculating the length of cutoff geodesic line, and the results match perturbative CFT results [22, 24]. The entanglement entropy in $T\bar{T}$ deformation was also studied on both the field theory side and holographic side in recent works [51–55]. We prefer to use the mixed boundary condition perspective to study holographic entanglement entropy. Since

the deformed geometry is still AdS_3 , we will work in the $SL(2, \mathbb{R}) \times SL(2, \mathbb{R})$ gauged Chern-Simons formalism of AdS_3 [56]. The Chern-Simons formalism has been used to study $T\bar{T}$ deformation in the literatures [47–49, 57–59]. In the gauge theory form, the holographic entanglement entropy is encoded in the Wilson line of Chern-Simons [60], see also [61, 62]. The Wilson lines are also related to the bulk geometry [63, 64]. Generally, the Wilson lines depend on the path and representation of the gauge group. If we choose a appropriate representation of $\mathfrak{sl}(2, \mathbb{R})$, the trace over the representation can be formulated into the path integral of a $SL(2, \mathbb{R}) \times SL(2, \mathbb{R})$ invariant auxiliary theory. The on-shell action of the auxiliary is equivalent to the length of geodesics in AdS_3 . In addition, the Wilson line is a probe in gauge theory, just like a point particle in a curved background. The Wilson lines give a back-reaction to the bulk geometry, and the resulting geometry turns out to be a conical defect on the branch point, which exactly generates a n -sheet manifold [60, 62]. Therefore, the Wilson line back reaction corresponds to the replica trick along the ending points of the Wilson line on the boundary. These results told us that the Wilson line is related to the entanglement entropy through

$$S_{\text{EE}} = -\log(W_{\mathcal{R}}(C)),$$

where the ending points of the Wilson line correspond to the interval on the boundary. The thermal entropy also turned out corresponds to the Wilson loop. We use this technique for the deformed AdS_3 geometry. The single interval holographic entanglement entropy is calculated exactly, which can reproduce the perturbative result obtained in other literatures [22, 24, 54]. We also consider the two intervals entanglement entropy in $T\bar{T}$ deformation, which implies a certain phase transition. Moreover, the holographic entanglement entropy of $T\bar{T}$ -deformed AdS_3 in the non-perturbative region is also studied. The results show that the entanglement entropy behaves like a zero temperature CFT one for the large deformation parameter.

The paper is organized as follows: In section 2, we give an overview of the gravitational Wilson line approach to obtain the holographic entanglement entropy. In section 3, we introduce the deformed AdS_3 under $T\bar{T}$, which is parameterized by the deformed spectrum. The holographic entanglement entropy is obtained using the Wilson line approach. We also consider the two intervals entanglement entropy and its phase transition. The same result is derived by calculating the RT surface in the deformed AdS_3 in section 4. We summarize our results and discussion in section 5. The appendix contains our conventions and Wilson line defects.

2 Wilson lines and entanglement entropy in AdS_3

This section is a review of using the Wilson lines technique to calculate the holographic entanglement entropy, based on [60]. By rewriting the AdS_3 gravity in Chern-Simons form, the Wilson line in an infinite-dimensional representation of the bulk gauge group is related to the geodesics in the bulk. According to the Ryu-Takayanagi proposal [65, 66], the holographic entanglement entropy or RT surface can be obtained through the Wilson line approach.

2.1 Wilson lines in AdS₃ gravity

It is well-known that 3D general relativity has no local degrees of freedom, which is purely topological and can be formulated as a Chern-Simons theory [56]. In the case of AdS₃ gravity, the relevant Chern-Simons gauge group is $SO(2,2) \simeq SL(2, \mathbb{R}) \times SL(2, \mathbb{R})$, so Einstein-Hilbert action can be written as

$$S_{\text{EH}}[e, \omega] = I_{\text{CS}}[A] - I_{\text{CS}}[\bar{A}], \quad (2.1)$$

where the Chern-Simons action is

$$I_{\text{CS}}[A] = \frac{k}{4\pi} \int_{\mathcal{M}} \text{Tr} \left(A \wedge dA + \frac{2}{3} A \wedge A \wedge A \right), \quad k = \frac{1}{4G}. \quad (2.2)$$

The gauge fields A and \bar{A} are valued in $\mathfrak{sl}(2, \mathbb{R})$, which are the linear combination of gravitational vielbein and spin connection

$$A = (\omega^a + e^a) L_a, \quad \bar{A} = (\omega^a - e^a) L_a. \quad (2.3)$$

The L_a are $\mathfrak{sl}(2, \mathbb{R})$ generators, see Appendix A for our conventions. Variation of the action leads to the equations of motion

$$F \equiv dA + A \wedge A = 0, \quad \bar{F} \equiv d\bar{A} + \bar{A} \wedge \bar{A} = 0, \quad (2.4)$$

which are equivalent to the first order gravitational field equation and torsion free equation. The AdS₃ metric can also be recovered from the gauge fields via

$$g_{ij} = \frac{1}{2} \text{Tr} \left[(A_i - \bar{A}_i)(A_j - \bar{A}_j) \right]. \quad (2.5)$$

As a consequence, the AdS₃ gravity is formulated into a Chern-Simons gauge theory. By using the Chern-Simons form, we can introduce the gravitational Wilson lines in AdS₃ gravity

$$W_{\mathcal{R}}(C) = \text{Tr}_{\mathcal{R}} \left(\mathcal{P} \exp \int_C \mathcal{A} \right), \quad (2.6)$$

where \mathcal{R} denotes a representation of $\mathfrak{sl}(2, \mathbb{R})$, and C is a curve on \mathcal{M} with two ending points living on the boundary of \mathcal{M} . If the path C is closed, it gives the Wilson loop which is invariant under the gauge transformation

$$\mathcal{A} \rightarrow \mathcal{A}' = \Lambda^{-1}(d + \mathcal{A})\Lambda. \quad (2.7)$$

We can use the Wilson lines to probe the bulk geometry, instead of a massive particle. The massive particle moving in bulk is characterized by its mass m and spin s . These parameters would contribute to the backreaction on the bulk geometry. The trajectory of the particle can be understood as geodesics. When we turn to use the Wilson line to probe the bulk geometry, we have to use the infinite-dimensional representations of $\mathfrak{sl}(2, \mathbb{R})$, characterized

by (h, \bar{h}) . So that the mass m and spin s of the particle can be encoded in the representation of $\mathfrak{sl}(2, \mathbb{R})$ through the relations $m = h + \bar{h}$ and $s = h - \bar{h}$. For the representation of $\mathfrak{sl}(2, \mathbb{R})$ see Appendix A.

Note that infinite-dimensional representations of symmetry algebras can be regarded as the Hilbert spaces of quantum mechanical systems in physics. The trace over all the states in the representation \mathcal{R} can be formulated into a path integral of an auxiliary quantum mechanical system. Then the Wilson line can be written as

$$W_{\mathcal{R}}(C) = \int \mathcal{D}U \exp[-S(U; \mathcal{A})_C]. \quad (2.8)$$

where $S(U; \mathcal{A})_C$ is the action of the auxiliary quantum mechanical system that lives on the Wilson line. The action should have a global symmetry group $SL(2, \mathbb{R}) \times SL(2, \mathbb{R})$, so that the Hilbert space of the system will be precisely the representation of $\mathfrak{sl}(2, \mathbb{R})$ after quantization.

For the free theory (without gauge fields), an appropriate system is described by a particle moving on the group manifold [67], whose action reads

$$S(U, P)_{\text{free}} = \int_C ds \left(\text{Tr} \left(PU^{-1} \frac{dU}{ds} \right) + \lambda(s) (\text{Tr} (P^2) - \mathcal{C}) \right), \quad (2.9)$$

where P lives in the Lie algebra $\mathfrak{sl}(2, \mathbb{R})$ and U lives in Lie group $SL(2, \mathbb{R})$. The trace in this action means contraction with Cartan-Killing metric. The equations of motion for the free theory are

$$U^{-1} \frac{dU}{ds} + 2\lambda P = 0, \quad (2.10)$$

$$\frac{dP}{ds} = 0, \quad (2.11)$$

$$\text{Tr} P^2 = \mathcal{C}. \quad (2.12)$$

This action has a $SL(2, \mathbb{R}) \times SL(2, \mathbb{R})$ global symmetry, namely under the following global gauge transformation

$$U(s) \rightarrow LU(s)R, \quad P(s) \rightarrow R^{-1}P(s)R, \quad L, R \in SL(2, \mathbb{R}), \quad (2.13)$$

the action (2.9) is invariant.

In [60], it turns out that the system coupled with the external gauge fields A and \bar{A} should be

$$S(U, P; \mathcal{A})_C = \int_C ds \left(\text{Tr} (PU^{-1} D_s U) + \lambda(s) (\text{Tr} (P^2) - \mathcal{C}) \right), \quad (2.14)$$

where the covariant derivative is defined by

$$D_s U = \frac{d}{ds} U + A_s U - U \bar{A}_s, \quad A_s = A_\mu \frac{dx^\mu}{ds}. \quad (2.15)$$

The equations of motion become

$$U^{-1}D_sU + 2\lambda P = 0, \quad (2.16)$$

$$\frac{d}{ds}P + [\bar{A}_s, P] = 0, \quad (2.17)$$

$$\text{Tr } P^2 = \mathcal{C}. \quad (2.18)$$

After introducing the covariant derivative, the global symmetry (2.13) is enhanced to the local gauge symmetry. The action (2.14) is invariant under local gauge transformation

$$A_\mu \rightarrow L(x) (A_\mu + \partial_\mu) L^{-1}(x), \quad \bar{A}_\mu \rightarrow R^{-1}(x) (\bar{A}_\mu + \partial_\mu) R(x), \quad (2.19)$$

$$U(s) \rightarrow L(x^\mu(s))U(s)R(x^\mu(s)), \quad P(s) \rightarrow R(x^\mu(s))P(s)R(x^\mu(s)). \quad (2.20)$$

We have to point out that the equations of motion do not change under these gauge transformations. This feature is useful to construct the solutions of the equations of motion from the free theory solutions. If the gauge fields A and \bar{A} are pure gauge, the solutions for the equations (2.16)-(2.18) can be obtained from the free theory solution through the gauge transformation (2.19) and (2.20). We will treat more details in section 2.3.

2.2 Equivalence to the geodesic equation

This Wilson line probe should be equivalent to a massive particle moving in AdS_3 . Then we will show that the usual geodesic equation with respect to the metric would appear in the Wilson line path. We denote the Wilson line path in the bulk by $x^\mu(s)$. Using the classical equation of motion (2.16)-(2.18), the action (2.14) can be reduced into a second order one

$$S(U; A, \bar{A})_C = \sqrt{\mathcal{C}} \int_C ds \sqrt{\text{Tr} (U^{-1}D_sU)^2}. \quad (2.21)$$

In this form, the action is essentially a gauged sigma model, whose equation of motion reads

$$\frac{d}{ds} \left((A^u - \bar{A})_\mu \frac{dx^\mu}{ds} \right) + [\bar{A}_\mu, A_\nu^u] \frac{dx^\mu}{ds} \frac{dx^\nu}{ds} = 0, \quad (2.22)$$

where

$$A_s^u = U^{-1} \frac{d}{ds} U + U^{-1} A_s U. \quad (2.23)$$

For the given gauge fields (A, \bar{A}) , the equation of motion depends on the choice of path $x^\mu(s)$. From the perspective of the equation of motion, we learn that $U(s)$ acts like a gauge transformation on the connection A . There is a good choice for $U(s)$, so that the particle does not move in the auxiliary space, i.e. $U(s) = \mathbf{1}$. In this case, the equation of motion reduces to

$$\frac{d}{ds} \left(e_\mu^a \frac{dx^\mu}{ds} \right) + \omega_{\mu b}^a e_\nu^b \frac{dx^\mu}{ds} \frac{dx^\nu}{ds} = 0. \quad (2.24)$$

This is precisely the geodesic equation for the curve $x^\mu(s)$ on a spacetime with vielbein and spin connection which is equivalent to the more familiar Christoffel symbols forms. Furthermore, the on-shell the action (2.14) for $U(s) = \mathbf{1}$ becomes

$$S(U; A, \bar{A})_C = \sqrt{2\mathcal{C}} \int_C ds \sqrt{g_{\mu\nu}(x) \frac{dx^\mu}{ds} \frac{dx^\nu}{ds}}, \quad (2.25)$$

which is manifestly the proper distance along the geodesic.

We have learned that the Wilson line in AdS₃ gravity can be expressed as a path integral of an auxiliary quantum mechanical system, whose action is (2.14). The on-shell action turns out to be the proper distance along the geodesic. Thus in the classical limit, one can find that the value of the Wilson line

$$W_{\mathcal{R}}(x_i, x_f) = \exp(-\sqrt{2\mathcal{C}}L(x_i, x_f)), \quad (2.26)$$

where $L(x_i, x_f)$ is the length of the bulk geodesic connecting these two endpoints on the boundary. Holographically, it was proposed by Ryu and Takayanagi that the field-theoretical entanglement entropies correspond to the length of the bulk geodesics ending on the boundary [65, 66]. In terms of the Chern-Simons description of AdS₃ gravity, we can calculate the entanglement entropy from the Wilson line

$$S_{\text{EE}} = -\log(W_{\mathcal{R}}(C)). \quad (2.27)$$

In [60], it was also shown that the Wilson line backreaction on the geometry would create a non-trivial holonomy, which can be interpreted as the conical singularity in the bulk. The conical defects hence reproduce the field-theoretical entanglement entropy formula. In the later of this paper, we would like to use the Wilson line technique to compute the holographic entanglement entropy in Chern-Simons AdS₃ gravity, including the $T\bar{T}$ -deformed AdS₃.

2.3 Holographic entanglement entropy

In this section, we calculate $W_{\mathcal{R}}(C)$ with C ending on the AdS₃ boundary at two points denoted by $x_i = x(s_i), x_f = x(s_f)$. Classically, we just need to calculate the on-shell action of the auxiliary system

$$S_{\text{on-shell}} = \int_C ds \text{Tr} (PU^{-1}D_s U) = -2\mathcal{C} \int_{s_i}^{s_f} ds \lambda(s), \quad (2.28)$$

which depends on the solution of the equations of motion. The solutions can be constructed from the free theory solutions, i.e. (2.10)-(2.12), through the gauge transformation (2.19) and (2.20). First of all, we should note the solutions to free theory, denoting them by $U_0(s)$ and P_0 , are

$$U_0(s) = u_0 \exp(-2\alpha(s)P_0), \quad \text{with} \quad \frac{d\alpha(s)}{ds} = \lambda(s), \quad (2.29)$$

where P_0 and u_0 are constant. Next, we assume the bulk gauge fields are in pure gauge

$$A = L(x)dL^{-1}(x), \quad \bar{A} = R^{-1}(x)dR(x). \quad (2.30)$$

In fact, most of the AdS₃ solutions are in pure gauge, such as BTZ black hole and Banãodos geometry. Then one can verify the following is the classical solution of (2.16)-(2.18)

$$U(s) = L(x(s))U_0(s)R(x(s)), \quad P(s) = R^{-1}(x(s))P_0R(x(s)). \quad (2.31)$$

These solutions are directly obtained from the local gauge symmetry of the equations of motion. As argued in [60], the boundary conditions for $U(s)$ on the boundary ending points can be chosen as

$$U(s_i) = L(x(s_i))u_0 \exp(-2\alpha(s_i)P_0)R(x(s_i)) = \mathbf{1}, \quad (2.32)$$

$$U(s_f) = L(x(s_f))u_0 \exp(-2\alpha(s_f)P_0)R(x(s_f)) = \mathbf{1}. \quad (2.33)$$

We then have to eliminate the initial value P_0 and u_0 . Solving u_0 from (2.32) and substituting into (2.33), one can find

$$\exp(-2\Delta\alpha P_0) = R(x(s_i))L(x(s_i))L^{-1}(x(s_f))R^{-1}(x(s_f)). \quad (2.34)$$

Taking the trace on both sides, we arrive at

$$\cosh\left(-2\Delta\alpha\sqrt{2\mathcal{C}}\right) = \frac{1}{2}\text{Tr}\left(R(x(s_i))L(x(s_i))L^{-1}(x(s_f))R^{-1}(x(s_f))\right), \quad (2.35)$$

where we have used

$$\text{Tr}(\exp(-2\Delta\alpha P_0)) = 2 \cosh\left(-2\Delta\alpha\sqrt{2\mathcal{C}}\right). \quad (2.36)$$

Finally, according to (2.27), we obtain the holographic entanglement entropy formula

$$S_{\text{EE}} = \sqrt{2\mathcal{C}} \cosh^{-1}\left[\frac{1}{2}\text{Tr}\left(R(x(s_i))L(x(s_i))L^{-1}(x(s_f))R^{-1}(x(s_f))\right)\right]. \quad (2.37)$$

We then use this formalism to check the holographic entanglement entropy in Poincare AdS₃ and BTZ black hole.

2.3.1 Poincaré AdS₃

For the case of Poincare AdS₃, the line element reads

$$ds^2 = \frac{dr^2}{r^2} + r^2(d\theta^2 - dt^2). \quad (2.38)$$

In terms of the Chern-Simons gauge connection, this geometry is described by

$$A = \frac{dr}{r}L_0 + rL_1(d\theta + dt), \quad (2.39)$$

$$\bar{A} = -\frac{dr}{r}L_0 - rL_{-1}(d\theta - dt). \quad (2.40)$$

The gauge connections can be written in pure gauge form

$$A = LdL^{-1}, \quad L = \exp(-\ln r L_0) \exp(-(\theta + t)L_1), \quad (2.41)$$

$$\bar{A} = R^{-1}dR, \quad R = \exp((\theta - t)L_{-1}) \exp(-\ln r L_0). \quad (2.42)$$

In order to calculate the entanglement entropy, we consider a time slice ($t = 0$) of this geometry and impose the following boundary conditions for the ending points of the Wilson line

$$r(s_i) = r(s_f) = r_0, \quad (2.43)$$

$$\Delta\theta = \theta(s_f) - \theta(s_i) = l, \quad (2.44)$$

which means we work on a constant radial boundary and the length of the interval is l . Plugging (2.41) and (2.42) into (2.37), one obtains

$$S_{\text{EE}} = \sqrt{2\mathcal{C}} \cosh^{-1} \left(1 + \frac{r_0^2 l^2}{2} \right). \quad (2.45)$$

Then taking the limit $r_0 \gg 1$, so that the result corresponds to the theory living on the conformal boundary, we arrive at ¹

$$S_{\text{EE}} = \frac{c}{3} \log \left(\frac{l}{\epsilon} \right). \quad (2.46)$$

where the UV cutoff of the boundary field theory corresponds to the radial cutoff in the bulk, and the central charge relates to the expectation value of Casimir

$$\epsilon = \frac{1}{r_0}, \quad \sqrt{2\mathcal{C}} = \frac{c}{6}. \quad (2.47)$$

The relation between the expectation value of Casimir and central charge can be derived by calculating the Wilson line defect, for the details see Appendix B. This result is exactly the entanglement entropy of CFT₂. The same answer can also be obtained by solving the bulk geodesic equation. However, in terms of the Wilson line form, we do not require the solution of any differential equations and follow from purely algebraic operations. This technique can be used for more complicated AdS₃ geometry.

2.3.2 BTZ black hole

For the BTZ black hole, the metric in Fefferman–Graham gauge is

$$ds^2 = \frac{dr^2}{r^2} + r^2 \left(dzd\bar{z} + \frac{1}{r^2} \mathcal{L}_0 dz^2 + \frac{1}{r^2} \bar{\mathcal{L}}_0 d\bar{z}^2 + \frac{1}{r^4} \mathcal{L}_0 \bar{\mathcal{L}}_0 dzd\bar{z} \right), \quad (2.48)$$

¹We have used the relation

$$\cosh^{-1}(x) \sim \log(2x) \quad \text{for } x \gg 1.$$

where \mathcal{L}_0 and $\bar{\mathcal{L}}_0$ are constants related to the mass and angular momentum of the black hole

$$\mathcal{L}_0 = \frac{M - J}{2}, \quad \bar{\mathcal{L}}_0 = \frac{M + J}{2}. \quad (2.49)$$

The corresponding Chern-Simons gauge connections read

$$A = \frac{dr}{r} L_0 + \left(r L_1 - \frac{1}{r} \mathcal{L}_0 L_{-1} \right) dz, \quad (2.50)$$

$$\bar{A} = -\frac{dr}{r} L_0 + \left(\frac{1}{r} \bar{\mathcal{L}}_0 L_1 - r L_{-1} \right) d\bar{z}. \quad (2.51)$$

In this case, one can obtain

$$L(r, z, \bar{z}) = \exp(-\ln r L_0) \exp(-z L_1 + \mathcal{L}_0 z L_{-1}), \quad (2.52)$$

$$R(r, z, \bar{z}) = \exp(\bar{\mathcal{L}}_0 \bar{z} L_1 - \bar{z} L_{-1}) \exp(-\ln r L_0). \quad (2.53)$$

In addition, such solutions can be parametrized as

$$A = b^{-1}(d + a)b, \quad \bar{A} = b(d + \bar{a})b^{-1}, \quad b = e^{\ln r L_0}, \quad (2.54)$$

Then a, \bar{a} are also flat connections, but do not depend on the radial coordinate

$$a = (L_1 - \mathcal{L}_0 L_{-1}) dz, \quad (2.55)$$

$$\bar{a} = (\bar{\mathcal{L}}_0 L_1 - L_{-1}) d\bar{z}. \quad (2.56)$$

Following the same steps in pure AdS₃ and the boundary conditions for the ending points of the Wilson line, we can get

$$\begin{aligned} & \text{Tr} \left(R(r_0, \theta(s_i), 0) L(r_0, \theta(s_i), 0) L^{-1}(r_0, \theta(s_f), 0) R^{-1}(r_0, \theta(s_f), 0) \right) \\ &= -2 \cosh(l\sqrt{\mathcal{L}_0}) \cosh(l\sqrt{\bar{\mathcal{L}}_0}) + \frac{(\mathcal{L}_0 \bar{\mathcal{L}}_0 + r_0^4) \sinh(l\sqrt{\mathcal{L}_0}) \sinh(l\sqrt{\bar{\mathcal{L}}_0})}{r_0^2 \sqrt{\mathcal{L}_0} \sqrt{\bar{\mathcal{L}}_0}} \\ &\sim \frac{r_0^2 \sinh(l\sqrt{\mathcal{L}_0}) \sinh(l\sqrt{\bar{\mathcal{L}}_0})}{\sqrt{\mathcal{L}_0} \sqrt{\bar{\mathcal{L}}_0}}, \quad (r_0 \gg 1) \end{aligned} \quad (2.57)$$

This result leads to the entanglement entropy

$$S_{\text{EE}} = \frac{c}{6} \log \left(\frac{r_0^2 \sinh(l\sqrt{\mathcal{L}_0}) \sinh(l\sqrt{\bar{\mathcal{L}}_0})}{\sqrt{\mathcal{L}_0} \sqrt{\bar{\mathcal{L}}_0}} \right). \quad (2.58)$$

If we consider the spinless black hole, i.e. $\mathcal{L}_0 = \bar{\mathcal{L}}_0$, the entanglement entropy reduces to

$$S_{\text{EE}} = \frac{c}{3} \log \left(\frac{\beta_0}{\pi \epsilon} \sinh \left(\frac{\pi l}{\beta_0} \right) \right), \quad \beta_0 = \frac{\pi}{\sqrt{\mathcal{L}_0}}, \quad (2.59)$$

where β_0 is the inverse temperature of the BTZ black hole [68–70]. This result coincides with the entanglement entropy of a CFT in thermal state.

2.4 Loops and thermal entropy

One can also consider the Wilson loops in AdS_3 . In this case, $W_{\mathcal{R}}(C)$ turns out to be the proper distance around the horizon, which corresponds to the black hole thermal entropy. We will then check it in the BTZ black hole. Consider the Wilson loop along the S_1 cycle $\theta \sim \theta + 2\pi$. In contrast to the open interval case, the closed path should be smooth and hence impose the periodic boundary condition

$$U(s_f) = U(s_i), \quad P(s_f) = P(s_i). \quad (2.60)$$

According to (2.31), the boundary condition for $P(s)$ implies

$$[P_0, R(s_i) R^{-1}(s_f)] = 0, \quad (2.61)$$

Hence, the boundary condition for $U(s)$ implies

$$\exp(-2\Delta\alpha P_0) = u_0^{-1} (L^{-1}(s_f) L(s_i)) u_0 (R(s_i) R^{-1}(s_f)). \quad (2.62)$$

In addition, note the relations

$$L^{-1}(s_f) L(s_i) = \exp\left(\oint d\theta a_\theta\right), \quad (2.63)$$

$$R(s_i) R^{-1}(s_f) = \exp\left(-\oint d\theta \bar{a}_\theta\right), \quad (2.64)$$

which are the holonomies of the connection, we can rewrite (2.62) as

$$\exp(-2\Delta\alpha P_0) = u_0^{-1} \exp(2\pi a_\theta) u_0 \exp(-2\pi \bar{a}_\theta). \quad (2.65)$$

Here we just consider the case of BTZ black hole, so that one can perform the simple integral over θ .

From (2.61), we learn that P_0 and \bar{a}_θ can be diagonalized simultaneously. If the initial value of u_0 is fixed, we can always choose a matrix V , such that a_θ can also be diagonalized by $u_0 V$

$$\begin{aligned} \exp(-2\Delta\alpha \lambda_P) &= (u_0 V)^{-1} \exp(2\pi a_\theta) u_0 V \exp(-2\pi \bar{\lambda}_\theta) \\ &= \exp(2\pi \lambda_\theta) \exp(-2\pi \bar{\lambda}_\theta), \end{aligned} \quad (2.66)$$

where λ_P , λ_θ and $\bar{\lambda}_\theta$ are diagonalized matrix of P_0 , a_θ and \bar{a}_θ . Contracting (2.66) with L_0 , we obtain the on-shell action for the loop

$$S_{\text{th}} = 2\pi\sqrt{2\mathcal{C}}\text{Tr}((\lambda_\theta - \bar{\lambda}_\theta)L_0). \quad (2.67)$$

For the BTZ black hole, the diagonalized gauge connections are

$$\lambda_\theta = 2\sqrt{\mathcal{L}_0}L_0, \quad \bar{\lambda}_\theta = -2\sqrt{\mathcal{L}_0}L_0. \quad (2.68)$$

Finally, the Wilson loop gives precisely the entropy of the BTZ black hole

$$S_{\text{th}} = 2\pi\sqrt{\frac{c}{6}\mathcal{L}_0} + 2\pi\sqrt{\frac{c}{6}\bar{\mathcal{L}}_0}. \quad (2.69)$$

3 Holographic entanglement entropy in $T\bar{T}$ - deformed AdS_3

We turn to investigate the entanglement entropy of $T\bar{T}$ deformed CFTs from the gravity side. In [43], it is proposed that the holographic interpretation of $T\bar{T}$ deformed CFTs is still AdS_3 gravity but with the mixed boundary condition. The AdS_3 solutions associated with the mixed boundary condition can be obtained from the Bañados geometry through a coordinate transformation. As the deformed geometry is still AdS_3 , we prefer to work in Chern-Simons formulation. In this section, we introduce the $T\bar{T}$ deformed AdS_3 geometry. The holographic entanglement entropy of $T\bar{T}$ deformed CFTs can be obtained using the Wilson line technique in the deformed AdS_3 .

3.1 $T\bar{T}$ deformed AdS_3 geometry

We start from the general AdS_3 solution with a flat conformal boundary, which is called the Bañados geometry [71]. In Fefferman-Graham gauge, the line element reads

$$ds^2 = \frac{dr^2}{r^2} + r^2 \left(dzd\bar{z} + \frac{1}{r^2} \mathcal{L}(z) dz^2 + \frac{1}{r^2} \bar{\mathcal{L}}(\bar{z}) d\bar{z}^2 + \frac{1}{r^4} \mathcal{L}(z) \bar{\mathcal{L}}(\bar{z}) dzd\bar{z} \right), \quad (3.1)$$

The parameters $\mathcal{L}(z)$ and $\bar{\mathcal{L}}(\bar{z})$ are arbitrary holomorphic and antiholomorphic functions, which are related to the energy and angular momentum

$$\mathcal{L} = \frac{E + J}{2}, \quad \bar{\mathcal{L}} = \frac{E - J}{2}. \quad (3.2)$$

The corresponding Chern-Simons gauge fields are

$$A = \frac{dr}{r} L_0 + \left(r L_1 - \frac{1}{r} \mathcal{L}(z) L_{-1} \right) dz, \quad (3.3)$$

$$\bar{A} = -\frac{dr}{r} L_0 - \left(\frac{1}{r} \bar{\mathcal{L}}(\bar{z}) L_1 - r L_{-1} \right) d\bar{z}. \quad (3.4)$$

In this sense, the deformed Bañados geometry can be constructed through a field-dependent coordinate transformation [43], which reads

$$dz = \frac{1}{1 - \mu^2 \mathcal{L}_\mu \bar{\mathcal{L}}_\mu} (dw - \mu \bar{\mathcal{L}}_\mu d\bar{w}), \quad d\bar{z} = \frac{1}{1 - \mu^2 \mathcal{L}_\mu \bar{\mathcal{L}}_\mu} (d\bar{w} - \mu \mathcal{L}_\mu dw), \quad (3.5)$$

where μ is the deformation parameter. One should note that the parameters \mathcal{L} and $\bar{\mathcal{L}}$ in (3.1) would turn into \mathcal{L}_μ and $\bar{\mathcal{L}}_\mu$ under the coordinate transformation. Generally, the parameters \mathcal{L}_μ and $\bar{\mathcal{L}}_\mu$ are different from the undeformed ones \mathcal{L} and $\bar{\mathcal{L}}$. The relations between deformed parameters $\mathcal{L}_\mu, \bar{\mathcal{L}}_\mu$ and undeformed parameters $\mathcal{L}, \bar{\mathcal{L}}$ can be fixed by two ways. The first one is that the deformation smoothly changes the spectrum but does not change the local degeneracy of states. Therefore, in the bulk, this implies that the $T\bar{T}$

deformation does not change the horizon area of a black hole. The second one is that the deformed geometry can be transformed into the undeformed one without changing the periodicity of the spatial coordinate. Indeed, the transformation is different from the inverse of (3.5). These considerations lead to

$$\frac{\mathcal{L}_\mu(1 - \mu\bar{\mathcal{L}}_\mu)^2}{(1 - \mu^2\mathcal{L}_\mu\bar{\mathcal{L}}_\mu)^2} = \mathcal{L}, \quad \frac{\bar{\mathcal{L}}_\mu(1 - \mu\mathcal{L}_\mu)^2}{(1 - \mu^2\mathcal{L}_\mu\bar{\mathcal{L}}_\mu)^2} = \bar{\mathcal{L}}. \quad (3.6)$$

One can turn to [43] for more details about fixing these relations.

By using the coordinate transformation (3.5), we obtain the deformed Chern-Simons gauge fields

$$A = \frac{1}{r}L_0dr + \frac{1}{1 - \mu^2\mathcal{L}_\mu\bar{\mathcal{L}}_\mu} \left(rL_1 - \frac{1}{r}\mathcal{L}_\mu L_{-1} \right) (dw - \mu\bar{\mathcal{L}}_\mu d\bar{w}), \quad (3.7)$$

$$\bar{A} = -\frac{1}{r}L_0dr - \frac{1}{1 - \mu^2\mathcal{L}_\mu\bar{\mathcal{L}}_\mu} \left(\frac{1}{r}\bar{\mathcal{L}}_\mu L_1 - rL_{-1} \right) (d\bar{w} - \mu\mathcal{L}_\mu dw). \quad (3.8)$$

Note that $\mathcal{L}(z)$ and $\bar{\mathcal{L}}(\bar{z})$ correspond to the charges of the solution in the Bañados geometry. However, in the deformed geometry, the parameters $\mathcal{L}(z)$ and $\bar{\mathcal{L}}(\bar{z})$ do not correspond to the charges. Indeed, the deformed energy and angular momentum can be obtained from both field theory and gravity side

$$E_\mu = \frac{1}{\mu} \left(1 - \sqrt{1 - 2\mu(\mathcal{L} + \bar{\mathcal{L}}) + \mu^2(\mathcal{L} - \bar{\mathcal{L}})^2} \right), \quad J_\mu = J. \quad (3.9)$$

Analogous to (3.2), we introduce the new parameters

$$\mathcal{Q} = \frac{E_\mu + J_\mu}{2} = \frac{1}{2\mu} \left[1 + \mu(\mathcal{L} - \bar{\mathcal{L}}) - \sqrt{1 - 2\mu(\mathcal{L} + \bar{\mathcal{L}}) + \mu^2(\mathcal{L} - \bar{\mathcal{L}})^2} \right], \quad (3.10)$$

$$\bar{\mathcal{Q}} = \frac{E_\mu - J_\mu}{2} = \frac{1}{2\mu} \left[1 - \mu(\mathcal{L} - \bar{\mathcal{L}}) - \sqrt{1 - 2\mu(\mathcal{L} + \bar{\mathcal{L}}) + \mu^2(\mathcal{L} - \bar{\mathcal{L}})^2} \right]. \quad (3.11)$$

We can regard \mathcal{Q} and $\bar{\mathcal{Q}}$ as the generalized parameters of \mathcal{L} and $\bar{\mathcal{L}}$ in the deformed geometry, and \mathcal{Q} and $\bar{\mathcal{Q}}$ reduce to \mathcal{L} and $\bar{\mathcal{L}}$ in the limit $\mu \rightarrow 0$. We find it is more convenient to parametrize the deformed gauge fields or metric in terms of these two independent charges. In terms of these charges, the Chern-Simons gauge connections are formulated as

$$A = \frac{dr}{r}L_0 + \frac{1 - \mu\mathcal{Q}}{1 - \mu(\mathcal{Q} + \bar{\mathcal{Q}})} \left(r(1 - \mu\bar{\mathcal{Q}})L_1 - \frac{1}{r}\mathcal{Q}L_{-1} \right) dw - \frac{\mu\bar{\mathcal{Q}}}{1 - \mu(\mathcal{Q} + \bar{\mathcal{Q}})} \left(r(1 - \mu\bar{\mathcal{Q}})L_1 - \frac{1}{r}\mathcal{Q}L_{-1} \right) d\bar{w}, \quad (3.12)$$

$$\bar{A} = -\frac{dr}{r}L_0 + \frac{\mu\mathcal{Q}}{1 - \mu(\mathcal{Q} + \bar{\mathcal{Q}})} \left(\frac{1}{r}\bar{\mathcal{Q}}L_1 - r(1 - \mu\mathcal{Q})L_{-1} \right) dw - \frac{1 - \mu\bar{\mathcal{Q}}}{1 - \mu(\mathcal{Q} + \bar{\mathcal{Q}})} \left(\frac{1}{r}\bar{\mathcal{Q}}L_1 - r(1 - \mu\mathcal{Q})L_{-1} \right) d\bar{w}, \quad (3.13)$$

In the following, we prefer to use the coordinates $\theta = (w + \bar{w})/2, t = (w - \bar{w})/2$, where t represents the time direction while θ denotes the spatial coordinate at the boundary with the identification $\theta \sim \theta + 2\pi$. We then have

$$A_r = \frac{1}{r}L_0, \quad A_\theta = r(1 - \mu\bar{\mathcal{Q}})L_1 - \frac{1}{r}\mathcal{Q}L_{-1}, \quad A_t = K\left(r(1 - \mu\bar{\mathcal{Q}})L_1 - \frac{1}{r}\mathcal{Q}L_{-1}\right), \quad (3.14)$$

$$\bar{A}_r = -\frac{1}{r}L_0, \quad \bar{A}_\theta = \frac{1}{r}\bar{\mathcal{Q}}L_1 - r(1 - \mu\mathcal{Q})L_{-1}, \quad \bar{A}_t = \bar{K}\left(\frac{1}{r}\bar{\mathcal{Q}}L_1 - r(1 - \mu\mathcal{Q})L_{-1}\right), \quad (3.15)$$

where

$$K = \frac{1 + \mu(\bar{\mathcal{Q}} - \mathcal{Q})}{1 - \mu(\mathcal{Q} + \bar{\mathcal{Q}})}, \quad \bar{K} = -\frac{1 - \mu(\bar{\mathcal{Q}} - \mathcal{Q})}{1 - \mu(\mathcal{Q} + \bar{\mathcal{Q}})}. \quad (3.16)$$

The radial gauge (2.54) still holds for the deformed gauge fields, so that the induced gauge connections are

$$a_\theta = (1 - \mu\bar{\mathcal{Q}})L_1 - \mathcal{Q}L_{-1}, \quad a_t = K\left((1 - \mu\bar{\mathcal{Q}})L_1 - \mathcal{Q}L_{-1}\right), \quad (3.17)$$

$$\bar{a}_\theta = \bar{\mathcal{Q}}L_1 - (1 - \mu\mathcal{Q})L_{-1}, \quad \bar{a}_t = \bar{K}\left(\bar{\mathcal{Q}}L_1 - (1 - \mu\mathcal{Q})L_{-1}\right). \quad (3.18)$$

In addition, we can also write down the deformed

$$ds^2 = \frac{dr^2}{r^2} + \frac{1}{r^2(1 - \mu(\mathcal{Q} + \bar{\mathcal{Q}}))^2} \times \\ \left(\mathcal{Q}(1 - \mu\mathcal{Q})(1 - \mu r^2)dw + \left(\mu\mathcal{Q}\bar{\mathcal{Q}} + r^2(1 - \mu\mathcal{Q})(1 - \mu\bar{\mathcal{Q}})\right)d\bar{w}\right) \times \\ \left(\bar{\mathcal{Q}}(1 - \mu\bar{\mathcal{Q}})(1 - \mu r^2)d\bar{w} + \left(\mu\mathcal{Q}\bar{\mathcal{Q}} + r^2(1 - \mu\mathcal{Q})(1 - \mu\bar{\mathcal{Q}})\right)dw\right). \quad (3.19)$$

We will use the deformed geometry to calculate the holographic entanglement entropy in the $T\bar{T}$ deformed CFTs. For simplicity, we just consider the constant charges \mathcal{Q} and $\bar{\mathcal{Q}}$, namely we work in $T\bar{T}$ deformed BTZ black hole.

3.2 $T\bar{T}$ -deformed holographic entanglement entropy

For the $T\bar{T}$ -deformed AdS_3 , the metric still satisfies the Einstein equation or flat connection condition in the Chern-Simons theory although it takes a complicated form. In the Poincaré AdS_3 , the Wilson line would produce a back-reaction in the bulk geometry. The back-reaction would then lead to a conical defect on the ending points of Wilson line, which generates the n -sheet manifold on the boundary. According to the replica trick on the boundary field theory, the Wilson line exactly leads to the entanglement entropy. One can turn to Appendix B for details. We can always transform the $T\bar{T}$ -deformed AdS_3 solution into the Poincaré form [72, 73]. However, the temperature (the period of Euclidean time) in deformed AdS_3 is different from the original one. The crucial point is that we have to identify the deformed temperature and length of interval on the boundary under $T\bar{T}$ deformation.

We will treat these considerations in more details and obtain the $T\bar{T}$ deformed holographic entanglement entropy in this section.

Now, we can use the Wilson line technique to calculate the holographic entanglement entropy in $T\bar{T}$ -deformed AdS_3 . First of all, we can give a glance at the Poincaré AdS_3 , which turns out correspond to the zero temperature entanglement entropy. In Fefferman-Graham gauge, the Poincaré AdS_3 can be written as Bañados geometry (3.1) with \mathcal{L} and $\bar{\mathcal{L}}$ vanish. In this case, the bulk geometry is the same as the undeformed one, so the zero temperature entanglement entropy remains unchanged. This result coincides with the perturbative calculation in field theory and cutoff perspective in the bulk [22, 24].

We then consider the deformed BTZ black hole, in which the charges \mathcal{Q} and $\bar{\mathcal{Q}}$ are constants. For the deformed geometry, on a time slice, we obtain

$$\begin{aligned} L(r, \theta, t = 0) &= \exp(-\ln r L_0) \exp\left(-\int_{x_0}^x dx^i a_i\right) \\ &= \exp(-\ln r L_0) \exp\left(-\left(1 - \mu \bar{\mathcal{Q}}\right)\theta L_1 + \mathcal{Q}\theta L_{-1}\right), \end{aligned} \quad (3.20)$$

$$\begin{aligned} R(r, \theta, t = 0) &= \exp\left(\int_{x_0}^x dx^i \bar{a}_i\right) \exp(-\ln r L_0) \\ &= \exp\left(\bar{\mathcal{Q}}\theta L_1 - \left(1 - \mu \mathcal{Q}\right)\theta L_{-1}\right) \exp(-\ln r L_0). \end{aligned} \quad (3.21)$$

As the deformed geometries are still AdS_3 solution, we use the boundary condition for $U(s)$

$$U(s_i) = \mathbf{1}, \quad U(s_f) = \mathbf{1}, \quad (3.22)$$

as well as the same boundary conditions for the ending points of the Wilson line

$$r(s_i) = r(s_f) = r_0, \quad (3.23)$$

$$\Delta\theta = \theta(s_f) - \theta(s_i) = l. \quad (3.24)$$

We should point out that the boundary condition for U is actually the unique choice because of the Lorentz invariance at the boundary [60, 74]. As the $T\bar{T}$ deformation does not break Lorentz invariance, we can use the same boundary condition (3.22) for U . It seems that l is just the length of the interval in the deformed boundary. But it equals to the deformed length of interval, because the length is defined in the (w, \bar{w}) coordinates.

Using the gauge transformation (2.31), one can get the solution $U(s)$ for the Wilson line coupled to the deformed gauge fields. The boundary condition for $U(s)$ and ending points

boundary condition for the Wilson line imply

$$\begin{aligned}
& \text{Tr} \left((R(s_i) L(s_i)) (R(s_f) L(s_f))^{-1} \right) \\
&= 2 \cosh \left(l \sqrt{\bar{\mathcal{Q}}(1 - \mu \bar{\mathcal{Q}})} \right) \cosh \left(l \sqrt{\mathcal{Q}(1 - \mu \bar{\mathcal{Q}})} \right) \\
&+ \frac{r_0^2 \sqrt{\bar{\mathcal{Q}}(1 - \mu \bar{\mathcal{Q}})} \sqrt{\mathcal{Q}(1 - \mu \bar{\mathcal{Q}})} \sinh \left(l \sqrt{\bar{\mathcal{Q}}(1 - \mu \bar{\mathcal{Q}})} \right) \sinh \left(l \sqrt{\mathcal{Q}(1 - \mu \bar{\mathcal{Q}})} \right)}{\mathcal{Q} \bar{\mathcal{Q}}} \\
&+ \frac{\mathcal{Q} \bar{\mathcal{Q}} \sinh \left(l \sqrt{\bar{\mathcal{Q}}(1 - \mu \bar{\mathcal{Q}})} \right) \sinh \left(l \sqrt{\mathcal{Q}(1 - \mu \bar{\mathcal{Q}})} \right)}{r_0^2 \sqrt{\bar{\mathcal{Q}}(1 - \mu \bar{\mathcal{Q}})} \sqrt{\mathcal{Q}(1 - \mu \bar{\mathcal{Q}})}} \\
&\sim \frac{r_0^2 \sqrt{\bar{\mathcal{Q}}(1 - \mu \bar{\mathcal{Q}})} \sqrt{\mathcal{Q}(1 - \mu \bar{\mathcal{Q}})} \sinh \left(l \sqrt{\bar{\mathcal{Q}}(1 - \mu \bar{\mathcal{Q}})} \right) \sinh \left(l \sqrt{\mathcal{Q}(1 - \mu \bar{\mathcal{Q}})} \right)}{\mathcal{Q} \bar{\mathcal{Q}}}. \tag{3.25}
\end{aligned}$$

In the last step, we consider the $r_0 \gg 1$ limit. It is straightforward to get the holographic entanglement entropy for $T\bar{T}$ deformation

$$\begin{aligned}
S_{\text{EE}} &= \sqrt{2\mathcal{C}} \cosh^{-1} \left(\frac{r_0^2 \sqrt{\bar{\mathcal{Q}}(1 - \mu \bar{\mathcal{Q}})} \sqrt{\mathcal{Q}(1 - \mu \bar{\mathcal{Q}})} \sinh \left(l \sqrt{\bar{\mathcal{Q}}(1 - \mu \bar{\mathcal{Q}})} \right) \sinh \left(l \sqrt{\mathcal{Q}(1 - \mu \bar{\mathcal{Q}})} \right)}{2\mathcal{Q} \bar{\mathcal{Q}}} \right) \\
&\sim \frac{c}{6} \log \left(\frac{r_0^2 \sqrt{\bar{\mathcal{Q}}(1 - \mu \bar{\mathcal{Q}})} \sqrt{\mathcal{Q}(1 - \mu \bar{\mathcal{Q}})} \sinh \left(l \sqrt{\bar{\mathcal{Q}}(1 - \mu \bar{\mathcal{Q}})} \right) \sinh \left(l \sqrt{\mathcal{Q}(1 - \mu \bar{\mathcal{Q}})} \right)}{\mathcal{Q} \bar{\mathcal{Q}}} \right). \tag{3.26}
\end{aligned}$$

If the original geometry is non-rotating BTZ black hole, namely $\mathcal{Q} = \bar{\mathcal{Q}}$, the deformed entanglement entropy becomes

$$S_{\text{EE}} = \frac{c}{3} \log \left(\frac{r_0 \sqrt{\mathcal{Q}(1 - \mu \mathcal{Q})} \sinh \left(l \sqrt{\mathcal{Q}(1 - \mu \mathcal{Q})} \right)}{\mathcal{Q}} \right). \tag{3.27}$$

We then want to identify the deformed temperature. For the deformed BTZ black hole, the temperature can be obtained by analyzing the period of Euclidean time, which is discussed in the next section (equation (4.10)). We quote the result here

$$\beta = \frac{1}{T} = \frac{\pi(1 - 2\mu\mathcal{Q})}{\sqrt{\mathcal{Q}(1 - \mu\mathcal{Q})}}. \tag{3.28}$$

This temperature can also be derived using the first law of thermodynamics, and we will show it in section 3.3. For the limit $\mu \rightarrow 0$, the temperature reduces to the BTZ black hole temperature. The length of interval l is already the deformed one, which can be seen from the coordinate transformation (3.5) on a time slice. In terms of the deformed temperature,

we can express the entanglement entropy as

$$S_{\text{EE}} = \frac{c}{3} \log \left(\frac{\sqrt{\beta^2 + 4\mu\pi^2} + \beta}{2\pi\epsilon} \sinh \left(\frac{\pi l}{\sqrt{\beta^2 + 4\mu\pi^2}} \right) \right). \quad (3.29)$$

This is actually the $T\bar{T}$ deformed entanglement entropy obtained from the holographic approach. For $\mu = 0$, the deformed entanglement entropy reduces to the familiar entanglement entropy of CFT at finite temperature. For the small μ , we can obtain the perturbative result

$$S_{\text{EE}} = \frac{c}{3} \log \left(\frac{\beta}{\pi\epsilon} \sinh \left(\frac{\pi l}{\beta} \right) \right) + \frac{\mu c}{3} \left(\frac{\pi^2}{\beta^2} - \frac{2\pi^3 l}{\beta^3} \coth \left(\frac{\pi l}{\beta} \right) \right) + O(\mu^2). \quad (3.30)$$

In the ‘‘low temperature’’ limit $\beta \gg l$, up to the first order, the entanglement entropy becomes

$$S_{\text{EE-low}} = \frac{c}{3} \log \left(\frac{\beta}{\pi\epsilon} \sinh \left(\frac{\pi l}{\beta} \right) \right) + \frac{\mu c}{3} \left(\frac{\pi^2}{\beta^2} \right) + O(\mu^2). \quad (3.31)$$

In the ‘‘high temperature’’ limit $\beta \ll l$, the first order corrected entanglement entropy is

$$S_{\text{EE-high}} = \frac{c}{3} \log \left(\frac{\beta}{\pi\epsilon} \sinh \left(\frac{\pi l}{\beta} \right) \right) - \frac{2\mu c \pi^3 l}{3 \beta^3} \coth \left(\frac{\pi l}{\beta} \right) + O(\mu^2). \quad (3.32)$$

The ‘‘high temperature’’ result coincides with the result obtained from both boundary field side and AdS₃ with cutoff perspective [22, 24]². We apply the Wilson line approach to the $T\bar{T}$ -deformed AdS₃ and obtain the holographic entanglement entropy formula, which agree with the perturbation results. However, the ‘‘low temperature’’ result is different from the cutoff AdS₃ perspective.

We are more interested in the non-perturbative result. In order to make sure the entanglement entropy is real, we have

$$-\frac{\beta^2}{4\pi^2} < \mu, \quad (3.34)$$

which means the holographic description maybe loses when μ out of this region. For $\mu > 0$ the entanglement entropy is always real. In the following discussion, we just consider the $\mu > 0$ case, which also corresponds to the cutoff perspective. For a fixed temperature, we can consider the entanglement entropy for large deformation parameter

$$S_{\text{EE}} = \frac{c}{3} \log \left(\frac{l}{2\epsilon} \right) + \frac{\beta c}{6\pi} \frac{1}{\sqrt{\mu}} + \left(\frac{cl^2}{72} - \frac{\beta^2 c}{24\pi^2} \right) \frac{1}{\mu} + O \left(\frac{1}{\mu} \right). \quad (3.35)$$

²Note that our convention is different from Ref. [22]. In [22], the deformation parameter is related to the radial cutoff $r_c^2 = \frac{6}{\mu\pi c}$, while we have $r_c^2 = \frac{1}{\mu}$ in this paper. Therefore, if one replaces μ by $\frac{\mu\pi c}{6}$, the equation (3.32) becomes

$$S_{\text{EE-high}} = \frac{c}{3} \log \left(\frac{\beta}{\pi\epsilon} \sinh \left(\frac{\pi l}{\beta} \right) \right) - \frac{\mu\pi^4 c^2 l}{9\beta^3} \coth \left(\frac{\pi l}{\beta} \right). \quad (3.33)$$

which is exactly the result in [22].

The leading order coincides with the entanglement entropy of the zero temperature CFT with the length of interval $l/2$. Therefore the holographic entanglement entropy has nothing to do with the temperature for large deformation parameter. However, we can not directly see this feature from the cutoff perspective, the reason is that the cutoff surface would move into the horizon for large deformation parameter at a fixed finite temperature. In order to see this feature from cutoff perspective, we have to consider the holographic entanglement entropy at the high temperature limit, so that we can keep the cutoff surface outside the horizon even for large deformation parameter. In this case, we first take the high temperature limit and then consider the large deformation parameter limit. For the high temperature limit, the entanglement entropy (3.28) becomes

$$S_{\text{EE}} = \frac{c}{3} \log \left(\frac{\sqrt{\mu}}{\epsilon} \sinh \left(\frac{l}{2\sqrt{\mu}} \right) \right) + \frac{c\beta}{6\pi\sqrt{\mu}} + O(\beta^2). \quad (3.36)$$

This formula leads to (3.35) for the large deformation parameter as well. These results imply the $T\bar{T}$ deformation behaves like the free theory at the large μ limit. The similar feature was also found in [75, 76], in which the authors shown that at the level of the equations of motion the left- and right-chiral sectors of $T\bar{T}$ deformed free theories are decoupled when the deformation parameter is sent to infinity.

For the holographic entanglement entropy in BTZ black hole, it turns out that there will be a phase transition when the interval becomes larger [65, 66]. The similar phase transition are also exist in $T\bar{T}$ -deformed BTZ black hole. As the size of interval becomes larger, we find the deformed holographic entanglement entropy becomes

$$S_{\text{EE}} \sim \frac{c\pi l}{3} \frac{1}{\sqrt{\beta^2 + 4\pi^2\mu}}, \quad (3.37)$$

which is proportional to the thermal entropy (3.48). This result can be interpreted as follows. In the presence of horizon, the RT surface (geodesic line) would approach the horizon and cover a part of the horizon when the size of interval becomes larger. Since the geodesic lines could wrap different parts of the horizon, there are two geodesics connecting the endpoints of the interval. The one being homologous to the boundary interval should be chosen to evaluate the holographic entanglement entropy, and the other geodesic is used to evaluate the entanglement entropy for the complementary interval

$$S'_{\text{EE}} = \frac{c}{3} \log \left(\frac{\sqrt{\beta^2 + 4\mu\pi^2} + \beta}{2\pi\epsilon} \sinh \left(\frac{\pi(2\pi - l)}{\sqrt{\beta^2 + 4\mu\pi^2}} \right) \right). \quad (3.38)$$

However, if $l > \pi$ the S'_{EE} is smaller than S_{EE} , but S'_{EE} is not homologous to the interval l . Similar to the BTZ black hole [77], we can construct another disconnected extremal surface by combining S'_{EE} and thermal entropy (3.48). Finally, the deformed entanglement entropy for a general interval is given by

$$S = \min\{S_{\text{EE}}, S'_{\text{EE}} + S_{\text{th}}\}. \quad (3.39)$$

Clearly, there is a phase transition between these two settings of extremal surface. In the high temperature limit and small deformation parameter, it turns out that the phase transition occurs at

$$l \sim 2\pi - \frac{\sqrt{\beta^2 + 4\mu\pi^2}}{2\pi} \log 2. \quad (3.40)$$

We show the phase transition of the holographic entanglement entropy is preserved under $T\bar{T}$ deformation.

Moreover, the Casini-Huerta entropic c -function [78] for the $T\bar{T}$ deformed entanglement entropy is

$$C(l, \mu) = l \frac{dS_{\text{EE}}}{dl} = \frac{\pi cl}{3\sqrt{\beta^2 + 4\pi^2\mu}} \coth\left(\frac{\pi l}{\sqrt{\beta^2 + 4\pi^2\mu}}\right), \quad (3.41)$$

which is always positive, and does not depend on the ultraviolet regulator. We also find that

$$\frac{\partial C(l, \mu)}{\partial l} = \frac{\pi c}{3} \left(\frac{\coth\left(\frac{\pi l}{\sqrt{\beta^2 + 4\pi^2\mu}}\right)}{\sqrt{\beta^2 + 4\pi^2\mu}} - \frac{\pi l \text{csch}^2\left(\frac{\pi l}{\sqrt{\beta^2 + 4\pi^2\mu}}\right)}{\beta^2 + 4\pi^2\mu} \right) \geq 0, \quad (3.42)$$

which implies the entropic c -function is non-decreasing along the renormalization group flow towards the ultraviolet. The similar result was also found in single trace $T\bar{T}$ deformation [79].

3.3 Thermal entropy

The thermal entropy of the deformed BTZ black hole can also be calculated from the Wilson loop. As discussed in section 2.4, the thermal entropy can be obtained by diagonalizing the induced gauge connections a_θ and \bar{a}_θ in (3.17) and (3.18). For the deformed BTZ black hole, the diagonalized gauge connections read

$$\lambda_\theta = 2\sqrt{\mathcal{Q}(1 - \mu\bar{\mathcal{Q}})}L_0 = 2\sqrt{\bar{\mathcal{L}}}L_0, \quad (3.43)$$

$$\bar{\lambda}_\theta = -2\sqrt{\bar{\mathcal{Q}}(1 - \mu\mathcal{Q})}L_0 = -2\sqrt{\bar{\mathcal{L}}}L_0. \quad (3.44)$$

Finally, according to (2.67), we obtain the thermal entropy

$$S_{\text{th}} = 2\pi\sqrt{\frac{c}{6}\mathcal{L}} + 2\pi\sqrt{\frac{c}{6}\bar{\mathcal{L}}}, \quad (3.45)$$

which is the same as the BTZ black hole entropy. This result means the black hole entropy does not change under the $T\bar{T}$ deformation. On the field theory side, the degeneracy of states does not change under the $T\bar{T}$ flow.

For the deformed theory, the thermal entropy should be expressed in terms of the deformed energy. In case of $\mathcal{Q} = \bar{\mathcal{Q}}$, the entropy can be written as

$$S_{\text{th}} = 4\pi\sqrt{\frac{c}{6}\mathcal{Q}(1-\mu\mathcal{Q})} = 2\pi\sqrt{\frac{c}{6}E_\mu(2-\mu E_\mu)}, \quad (3.46)$$

which agrees with the result in [3]. The thermal entropy can help us to define the temperature in the $T\bar{T}$ -deformed theory. In fact, according to the first law of thermodynamics, the temperature can be determined by

$$T = \frac{\partial E_\mu}{\partial S_{\text{th}}} = \sqrt{\frac{6}{c}} \frac{\sqrt{\mathcal{Q}(1-\mu\mathcal{Q})}}{\pi(1-2\mu\mathcal{Q})} \sim \frac{\sqrt{\mathcal{Q}(1-\mu\mathcal{Q})}}{\pi(1-2\mu\mathcal{Q})}, \quad (3.47)$$

where we have used the convention $k = c/6 = 1$ in the definition of temperature. This is actually the temperature we have used in (3.28). The black hole thermal entropy can also be written in terms of temperature

$$S_{\text{th}} = \frac{c}{3} \frac{2\pi^2}{\sqrt{\beta^2 + 4\pi^2\mu}}. \quad (3.48)$$

3.4 Two intervals entanglement entropy

We proceed to consider the entanglement entropy of the system consists of two disjoint intervals. For the single interval case, we have shown that the entanglement entropy is the Wilson line or length of geodesic in AdS_3 with ending points on the spatial infinity boundary for both Brown-Henneaux boundary condition and mixed boundary condition. According to Ryu-Takayanagi's proposal [65, 66], we have two choices for how to draw the geodesics that end on the ending points of two intervals, which are shown in Figure 1. For each choice, the two intervals entanglement entropy decouples into a sum of single interval cases. The

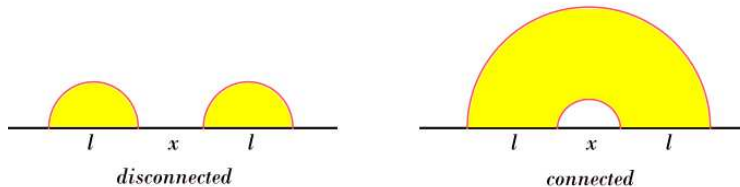


Figure 1: The two minimal surfaces for the two intervals boundary region. We consider the two intervals have the same length l separated by x . The left is the disconnected case, and the right is the connected case.

two intervals holographic entanglement entropy should be the minimal one of them

$$S_{\text{EE-2}} = \min\{S_{\text{dis}}, S_{\text{con}}\}. \quad (3.49)$$

This implies that there are two phases of the entanglement entropy. It turns out that there actually exist a phase transition between the connected and disconnected phase [80].

We first brief review the zero temperature entanglement entropy of two disjoint intervals. We assume the two intervals have the same length l separated by x , described in Figure 1. Then the difference between two phases is

$$\Delta S = S_{\text{dis}} - S_{\text{con}} = \frac{c}{3} \log \left(\frac{l^2}{x(2l+x)} \right). \quad (3.50)$$

One can find the phase transition critical point is determined by the cross-ratio

$$\eta = \frac{l^2}{(l+x)^2} = \frac{1}{2} \quad \text{or} \quad \frac{x}{l} = \sqrt{2} - 1. \quad (3.51)$$

For the finite temperature case, the similar phase transition was shown in [81, 82]. However, there is no quantity like cross-ratio to illustrate the critical point.

Now we would like to investigate the similar feature for the $T\bar{T}$ deformed entanglement entropy. For the different choices of Wilson lines or RT surfaces, we have

$$S_{\text{dis}} = \frac{c}{3} \log \left(\frac{\pi^2 \mu + \frac{1}{2} \beta \left(\sqrt{\beta^2 + 4\pi^2 \mu} + \beta \right)}{\pi^2 \epsilon^2} \sinh^2 \left(\frac{\pi l}{\sqrt{\beta^2 + 4\mu\pi^2}} \right) \right), \quad (3.52)$$

$$S_{\text{con}} = \frac{c}{3} \log \left(\frac{\pi^2 \mu + \frac{1}{2} \beta \left(\sqrt{\beta^2 + 4\pi^2 \mu} + \beta \right)}{\pi^2 \epsilon^2} \sinh \left(\frac{\pi x}{\sqrt{\beta^2 + 4\mu\pi^2}} \right) \sinh \left(\frac{\pi(2l+x)}{\sqrt{\beta^2 + 4\mu\pi^2}} \right) \right). \quad (3.53)$$

The two intervals entanglement entropy is the minimal one of them. In order to determine which is the minimal one and under what conditions the phase transition happens, we consider the difference between two RT surfaces

$$\Delta S = S_{\text{dis}} - S_{\text{con}} = \frac{c}{3} \log \left(\frac{\sinh^2 \left(\frac{\pi l}{\sqrt{\beta^2 + 4\mu\pi^2}} \right)}{\sinh \left(\frac{\pi x}{\sqrt{\beta^2 + 4\mu\pi^2}} \right) \sinh \left(\frac{\pi(2l+x)}{\sqrt{\beta^2 + 4\mu\pi^2}} \right)} \right). \quad (3.54)$$

This quantity is also related to the mutual information between two disjoint subsystems. From (3.54), we learn that ΔS behaves like the undeformed one but with different temperature. We first consider the low temperature and high temperature limit. For the low temperature limit $\beta \gg 1$, we have

$$\Delta S = \frac{c}{3} \log \left(\frac{l^2}{x(2l+x)} \right) + O(1/\beta^2). \quad (3.55)$$

The leading order is exactly the zero temperature case. The phase transition occurs at $x/l = \sqrt{2} - 1$ and does not depend on the deformation parameter. For the high temperature

limit $\beta \ll 1$, we have

$$\Delta S = \frac{c}{3} \log \left(\frac{\cosh \left(\frac{l}{\sqrt{\mu}} \right) - 1}{\cosh \left(\frac{l+x}{\sqrt{\mu}} \right) - \cosh \left(\frac{l}{\sqrt{\mu}} \right)} \right) + O(\beta^2). \quad (3.56)$$

In this case, the critical point depends on the deformation parameter.

We find it is convenient to introduce the following parameters

$$\tilde{l} = \frac{x}{l}, \quad \tilde{x} = \frac{x}{\beta}, \quad \tilde{\mu} = \frac{\mu}{\beta^2}. \quad (3.57)$$

In terms of the new parameters, the ΔS reduces to

$$\Delta S = \frac{c}{3} \log \left(\frac{\sinh^2 \left(\frac{\pi \tilde{x}}{\tilde{l} \sqrt{1+4\tilde{\mu}\pi^2}} \right)}{\sinh \left(\frac{\pi \tilde{x}}{\sqrt{1+4\tilde{\mu}\pi^2}} \right) \sinh \left(\frac{\pi(2+\tilde{l})\tilde{x}}{\tilde{l} \sqrt{1+4\tilde{\mu}\pi^2}} \right)} \right), \quad (3.58)$$

in which the temperature is implicit. We plot the critical lines $\Delta S = 0$ in (\tilde{l}, \tilde{x}) plane for different deformation parameters in Figure 2. Then we consider some special limit about

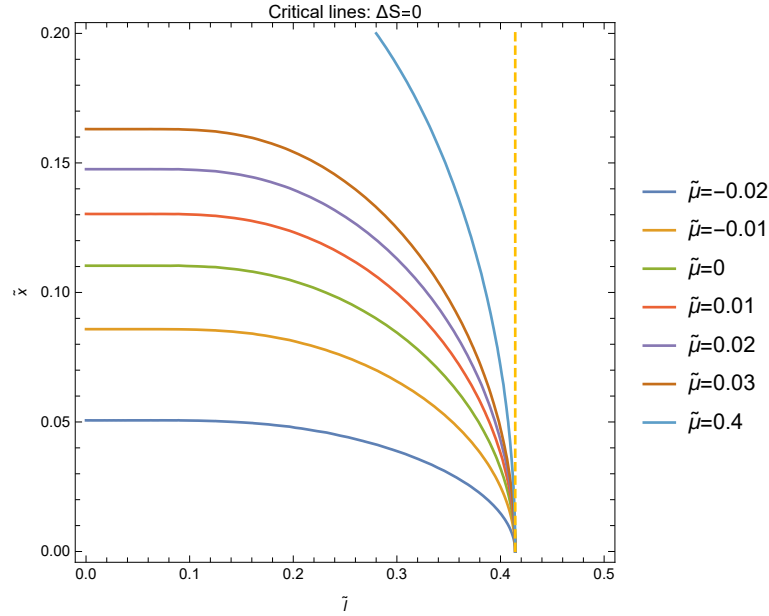


Figure 2: Plot the critical lines $\Delta S = 0$ in $\tilde{l} - \tilde{x}$ plane for different deformation parameters. The critical lines separate the connected phase (left side) and disconnected phase (right side). The green line corresponds to the undeformed case. The dashed line denotes the zero temperature critical line $\tilde{l} = \sqrt{2} - 1$. The critical lines tend to the zero temperature case with the increase of deformation parameter.

the critical lines. For $\tilde{x} \ll 1$, we have

$$\Delta S = \frac{c}{3} \left[\log \left(\frac{1}{\tilde{l}^2 + 2\tilde{l}} \right) - \frac{\pi^2(\tilde{l} + 1)^2 \tilde{x}^2}{3\tilde{l}^2(1 + 4\tilde{\mu}\pi^2)} \right] + O(\tilde{x}^3). \quad (3.59)$$

The leading order is just the zero temperature case and also does not depend on the deformation parameter. This result can be seen from Figure 2 that the critical lines coincide with the zero temperature one for small \tilde{x} .

It is interesting to investigate the μ dependence of phase transition. For the small $\tilde{\mu}$, there is actually exists a phase transition, which has been discussed in [24] using the perturbative method. We can also see from Figure 2 the critical line is around the undeformed case for both $\tilde{\mu} < 0$ and $\tilde{\mu} > 0$. For the $\tilde{\mu} \gg 1$ region, we have

$$\Delta S = \frac{c}{3} \log \left(\frac{1}{\tilde{l}^2 + 2\tilde{l}} \right) - \frac{c(\tilde{l} + 1)^2 \tilde{x}^2}{36\tilde{l}^2 \tilde{\mu}} + O(1/\tilde{\mu}^2). \quad (3.60)$$

The leading order is just the zero temperature case. One can also see from Figure 2 that the critical lines would become the zero temperature one as the increase of deformation parameters. This result implies the $T\bar{T}$ deformed theory becomes a decoupled free theory for large μ limit [75, 76].

These results show that there still exist the phase transition for two intervals entanglement entropy under $T\bar{T}$ deformation. The transition point is depends on the deformation parameter. The $T\bar{T}$ deformation does not introduce new phases. For large deformation parameter, the critical point is the same as zero temperature CFT case, it would be interesting to study this feature from the field theoretic results.

4 Geodesic line method

In this section we re-compute the holographic entanglement entropy in BTZ background with mix boundary condition using RT formula, i.e., identifying the holographic entanglement entropy as the geodesic distance. The results turn out to be consistent with the computation via Wilson line method.

The metric of BTZ black hole with mass M and angular momentum J takes the form (2.48).³ For simplicity we consider the case where the black hole being static $J = 0$. It follows from (3.6) that the deformed parameters $\mathcal{L}_\mu, \bar{\mathcal{L}}_\mu$ are constant and satisfy

$$\mathcal{L}_\mu = \bar{\mathcal{L}}_\mu = \frac{1 - \mu M \pm \sqrt{1 - 2\mu M}}{M\mu^2}, \quad (4.1)$$

where only the solution with “-” is well defined in $\mu \rightarrow 0$ limit. We start from the following metric

$$ds^2 = \frac{dr^2}{r^2} + r^2 \left(dzd\bar{z} + \frac{1}{r^2} (\mathcal{L}_\mu dz^2 + \bar{\mathcal{L}}_\mu d\bar{z}^2) + \frac{1}{r^4} \mathcal{L}_\mu \bar{\mathcal{L}}_\mu dzd\bar{z} \right), \quad (4.2)$$

³We follow the convention in [43], and set $4\pi G = 1, l = 1$ and $R = 2\pi$ (periodicity of spatial dimension) in their paper. We also use r which is related with the radial coordinate ρ in [43] as $r^2 = 1/\rho$. The cutoff in [43] locates at $\rho = \rho_c = \mu$, then in r -coordinate, $r_0 = r_c = 1/\sqrt{\mu}$.

in which we have replaced the $\mathcal{L}, \bar{\mathcal{L}}$ by $\mathcal{L}_\mu, \bar{\mathcal{L}}_\mu$ in the BTZ black hole solution, so that we can obtain the deformed BTZ only by using the coordinate transformation. Let $z = x + iy$, and define

$$r = \sqrt{\mathcal{L}_\mu} e^\rho, \quad x = \frac{\bar{x}}{\sqrt{4\mathcal{L}_\mu}}, \quad y = \frac{\bar{y}}{\sqrt{4\mathcal{L}_\mu}}, \quad (4.3)$$

then the metric becomes the global AdS₃

$$ds^2 = d\rho^2 + \cosh^2 \rho d\bar{x}^2 + \sinh^2 \rho d\bar{y}^2, \quad (4.4)$$

where \bar{y} is treated as the Euclidean time and \bar{x} the spatial coordinate. The requirement of no conical singularity in $\rho - \bar{y}$ plane implies the identification $\bar{y} \sim \bar{y} + 2\pi$, where the periodicity is related with the temperature for BTZ black hole. It is convenient to work in embedding coordinate

$$\begin{aligned} Y^0 &= \cosh \rho \cosh \bar{x}, & Y^3 &= \cosh \rho \sinh \bar{x}, \\ Y^1 &= \sinh \rho \sin \bar{y}, & Y^2 &= \sinh \rho \cos \bar{y}. \end{aligned} \quad (4.5)$$

In this coordinate system the BTZ black hole is a hypersurface $-(Y^0)^2 + (Y^3)^2 + (Y^1)^2 + (Y^2)^2 = -1$ in the background $ds^2 = -d(Y^0)^2 + d(Y^1)^2 + d(Y^2)^2 + d(Y^3)^2$. The geodesic distant d between two points Y_1^a, Y_2^b is simply computed by

$$\cosh d = -Y_1 \cdot Y_2 = Y_1^0 Y_2^0 - Y_1^1 Y_2^1 - Y_1^2 Y_2^2 - Y_1^3 Y_2^3. \quad (4.6)$$

The deformed metric corresponding to $T\bar{T}$ deformation can be obtained by transformation of

$$dz = \frac{1}{1 - \mu^2 \mathcal{L}_\mu \bar{\mathcal{L}}_\mu} (dw - \mu \bar{\mathcal{L}}_\mu d\bar{w}), \quad d\bar{z} = \frac{1}{1 - \mu^2 \mathcal{L}_\mu \bar{\mathcal{L}}_\mu} (d\bar{w} - \mu \mathcal{L}_\mu dw). \quad (4.7)$$

In the present case, (4.7) can be solved straightforwardly as

$$z = \frac{1}{1 - \mu^2 \mathcal{L}_\mu \bar{\mathcal{L}}_\mu} (w - \mu \bar{\mathcal{L}}_\mu \bar{w}), \quad \bar{z} = \frac{1}{1 - \mu^2 \mathcal{L}_\mu \bar{\mathcal{L}}_\mu} (\bar{w} - \mu \mathcal{L}_\mu w). \quad (4.8)$$

And its inverse

$$w = z + \mu \bar{\mathcal{L}}_\mu \bar{z}, \quad \bar{w} = \mu \mathcal{L}_\mu z + \bar{z}, \quad (4.9)$$

where $w = \theta + it, \bar{w} = \theta - it$. From the periodicity of \bar{y} discussed above, we can work out the period of t , which is

$$t \sim t + \frac{2\pi(1 - \mu \mathcal{L}_\mu)}{\sqrt{4\mathcal{L}_\mu}} = t + \beta, \quad \beta = \frac{\pi(1 - 2\mu \mathcal{Q})}{\sqrt{\mathcal{Q}(1 - \mu \mathcal{Q})}}, \quad (4.10)$$

where the β is the inverse temperature of deformed black hole, as well as the inverse temperature of the $T\bar{T}$ deformed CFT.

To compute the HEE of a single interval, we consider two ending points on the boundary locate at $(r_1, t_1, \theta_1) = (\sqrt{\mathcal{L}_\mu} e^{\rho_0}, 0, 0)$ and $(r_2, t_2, \theta_2) = (\sqrt{\mathcal{L}_\mu} e^{\rho_0}, 0, l)$ respectively. Then $w_1 = \bar{w}_1 = 0, w_2 = \bar{w}_2 = l$

$$z_1 = \bar{z}_1 = 0, \quad z_2 = \bar{z}_2 = \frac{l}{1 + \mu \mathcal{L}_\mu}. \quad (4.11)$$

In terms of embedding coordinates

$$Y_1^0 = \cosh \rho_0, \quad Y_1^3 = 0, \quad Y_1^1 = 0, \quad Y_1^2 = \sinh \rho_0, \quad (4.12)$$

and

$$Y_2^0 = \cosh \rho_0 \cosh \sqrt{4\mathcal{L}_\mu z_2}, \quad Y_2^3 = \cosh \rho \sinh \sqrt{4\mathcal{L}_\mu z_2}, \quad Y_2^1 = 0, \quad Y_2^2 = \sinh \rho_0. \quad (4.13)$$

Finally using (4.6), the geodesic distance between the points is

$$\begin{aligned} \cosh d &= \cosh^2 \rho_0 \cosh \sqrt{4\mathcal{L}_\mu z_2} - \sinh^2 \rho_0 \\ &= \frac{\mathcal{Q}}{2r_0^2(1-\mu\mathcal{Q})} \sinh^2 l \sqrt{\mathcal{Q}(1-\mu\mathcal{Q})} + \cosh^2 l \sqrt{\mathcal{Q}(1-\mu\mathcal{Q})} \\ &\quad + \frac{r_0^2(1-\mu\mathcal{Q})}{2\mathcal{Q}} \sinh^2 l \sqrt{\mathcal{Q}(1-\mu\mathcal{Q})}, \end{aligned} \quad (4.14)$$

where we made the replacement $\sqrt{\mathcal{L}_\mu z_2} = l \sqrt{\mathcal{Q}(1-\mu\mathcal{Q})}$. It follows that the HEE is

$$S_{\text{EE}} = \frac{1}{4G} \cosh^{-1} \left[\frac{\mathcal{Q}}{2r_0^2(1-\mu\mathcal{Q})} \sinh^2 l \sqrt{\mathcal{Q}(1-\mu\mathcal{Q})} + \cosh^2 l \sqrt{\mathcal{Q}(1-\mu\mathcal{Q})} + \frac{r_0^2(1-\mu\mathcal{Q})}{2\mathcal{Q}} \sinh^2 l \sqrt{\mathcal{Q}(1-\mu\mathcal{Q})} \right]. \quad (4.15)$$

For the $r_0 \rightarrow \infty$ limit, note the definition of temperature (4.10) and relation $1/4G = c/6$, we arrive at

$$S_{\text{EE}} = \frac{c}{3} \log \left(\frac{\sqrt{\beta^2 + 4\mu\pi^2} + \beta}{2\pi\epsilon} \sinh \left(\frac{\pi l}{\sqrt{\beta^2 + 4\mu\pi^2}} \right) \right), \quad \epsilon = \frac{1}{r_0}. \quad (4.16)$$

This coincides with (3.29) in the case of non-rotating BTZ black hole. We obtain the same holographic entanglement entropy formula by calculating the RT surface in the deformed BTZ black hole.

5 Conclusion and discussion

The $T\bar{T}$ deformed CFT was proposed dual to the AdS_3 with a certain mixed boundary condition. The AdS_3 with mixed boundary condition or the $T\bar{T}$ -deformed AdS_3 geometry can be obtained from the Banados geometry using the dynamical change of coordinates. In this paper, we studied the holographic entanglement entropy in the $T\bar{T}$ -deformed AdS_3 under this situation. In terms of Chern-Simons form, we derived the holographic entanglement entropy formula using the Wilson line technique. For the zero temperature case, the entanglement entropy turned out unchanged under the $T\bar{T}$ deformation. For the finite temperature case, we calculated the Wilson line with ending points on the boundary of

deformed AdS₃. After identifying the deformed temperature and length of interval on the boundary, we found the Wilson line lead to holographic entanglement entropy formula, which is closely related to the entanglement entropy in $T\bar{T}$ -deformed CFTs. The same formula was also obtained by calculating the RT surface in the $T\bar{T}$ -deformed BTZ black hole. The deformed entanglement entropy formula can reproduce the known perturbative results, which were obtained from both field theory and cutoff AdS₃ in other literature. We also showed that the entropic c-function is always positive and non-decreasing along the renormalization group flow towards the ultraviolet. For the non-perturbative region, our results show that the entanglement entropy behaves like entanglement entropy of CFT at zero temperature.

Moreover, we also considered the two intervals entanglement entropy and found there still exist a certain phase transition between disconnected and connected phase. It turned out that the critical point for the phase transition depends on the deformation parameters. The critical point is sensitive to the deformation parameter for the high temperature region. But the critical point becomes independent of deformation parameter for the low temperature region. For a fixed temperature, the critical point tends to the zero temperature case at large deformation parameter, which is shown in Figure 2.

Finally, we want to point out that the holographic entanglement entropy formula was derived from the holographic study and the formula agrees with the perturbative result. However, we still need an exact calculation from $T\bar{T}$ -deformed CFTs. In addition, since we found the entanglement entropy behaves like a free CFT, it would be interesting to study the $T\bar{T}$ deformation for large deformation parameter following [75, 76].

Acknowledgements

We are grateful to Song He for suggesting this topic. We would like to thank Yunfeng Jiang, Zhangcheng Liu, Hao Ouyang, Qiang Wen and Long Zhao for helpful discussions. This work is supported by the National Natural Science Foundation of China (No.12105113).

A Conventions

In this paper, we choose the following standard Lie algebra generators of $\mathfrak{sl}(2, \mathbb{R})$

$$L_{-1} = \begin{bmatrix} 0 & 1 \\ 0 & 0 \end{bmatrix}, \quad L_0 = \begin{bmatrix} \frac{1}{2} & 0 \\ 0 & -\frac{1}{2} \end{bmatrix}, \quad L_1 = \begin{bmatrix} 0 & 0 \\ -1 & 0 \end{bmatrix}, \quad (\text{A.1})$$

whose commutators simplify to

$$[L_a, L_b] = (a - b)L_{a+b}, \quad a, b \in \{0, \pm 1\}. \quad (\text{A.2})$$

The non-zero components of non-degenerate bilinear form are given by

$$\text{Tr}(L_0 L_0) = \frac{1}{2}, \quad \text{Tr}(L_{-1} L_1) = \text{Tr}(L_1 L_{-1}) = -1. \quad (\text{A.3})$$

We use the following representation of the $\mathfrak{sl}(2, \mathbb{R})$ Lie algebra, i.e. the highest-weight representation. The highest-weight state $|h\rangle$ satisfies

$$L_1|h\rangle = 0, \quad L_0|h\rangle = h|h\rangle. \quad (\text{A.4})$$

There is an infinite tower of descendant states found by acting with the raising operator

$$|h, n\rangle = (L_{-1})^n|h\rangle. \quad (\text{A.5})$$

These states form an irreducible, unitary, and infinite-dimensional representation of $\mathfrak{sl}(2, \mathbb{R})$. The quadratic Casimir operator of the algebra is

$$C = 2L_0^2 - (L_1L_{-1} + L_{-1}L_1), \quad (\text{A.6})$$

which commutes with all the elements of the algebra. The expectation value of Casimir operator on highest-weight state is

$$C = \langle h|C|h\rangle = 2h^2 - 2h. \quad (\text{A.7})$$

B Wilson line defects

The Wilson line as a probe in the bulk will produce a back-reaction in the bulk. To solve for this back-reaction, we consider the total action

$$S = S_{CS}[A] - S_{CS}[\bar{A}] + B + S(U; A, \bar{A})_C. \quad (\text{B.1})$$

where B denotes the boundary term, the last term is the auxiliary action associated with the Wilson line. For different boundary conditions, there will be different boundary terms. In case of the $T\bar{T}$ deformation, the boundary term turns out to be

$$B = \frac{k}{4\pi} \int_{\partial M} d^2x \frac{1}{\mu} \left(\sqrt{1 - 2\mu (\text{Tr}(A_\theta A_\theta) + \text{Tr}(\bar{A}_\theta \bar{A}_\theta)) + \mu^2 (\text{Tr}(A_\theta A_\theta) - \text{Tr}(\bar{A}_\theta \bar{A}_\theta))^2} - 1 \right). \quad (\text{B.2})$$

This boundary term leads to the $T\bar{T}$ deformed spectrum and can also help to reduce the gravitational action to $T\bar{T}$ deformed Alekseev-Shatashvili action on the boundary [48]. The boundary term does not contribute to the equation of motion, but the Wilson line term will contribute as a source for the equations of motion

$$\frac{k}{2\pi} F_{\mu\nu} = \int ds \frac{dx^\rho}{ds} \varepsilon_{\mu\nu\rho} \delta^{(3)}(x - x(s)) U P U^{-1}, \quad (\text{B.3})$$

$$\frac{k}{2\pi} \bar{F}_{\mu\nu} = - \int ds \frac{dx^\rho}{ds} \varepsilon_{\mu\nu\rho} \delta^{(3)}(x - x(s)) P. \quad (\text{B.4})$$

We can choose the Wilson line trajectory as a bulk geodesic, the corresponding Wilson line variables is

$$r(s) = s, \quad U(s) = \mathbf{1}, \quad P(s) = \sqrt{2\mathcal{C}} L_0. \quad (\text{B.5})$$

Contracting (B.3) and (B.4) with the tangent vector to the curve, we find the non-vanishing components of field strength F, \bar{F} are tangent to the curve

$$F_{\mu\nu} \frac{dx^\mu}{ds} = 0, \quad (\text{B.6})$$

$$\bar{F}_{\mu\nu} \frac{dx^\mu}{ds} = 0. \quad (\text{B.7})$$

Since we can always transform the AdS₃ solution into the Poincaré coordinate [72, 73], we just consider the Poincaré AdS₃. The solution is asymptotic AdS₃ in Poincaré coordinate

$$A = L(a_{\text{source}} + d)L^{-1}, \quad L = e^{-\ln r L_0} e^{-z L_1}, \quad (\text{B.8})$$

$$\bar{A} = R^{-1}(a_{\text{source}} + d)R, \quad R = e^{-\bar{z} L_{-1}} e^{-\ln r L_0}, \quad (\text{B.9})$$

where the coupling to the source is taken into account by

$$a_{\text{source}} = \sqrt{\frac{\mathcal{C}}{2}} \frac{1}{k} \left(\frac{dz}{z} - \frac{d\bar{z}}{\bar{z}} \right) L_0. \quad (\text{B.10})$$

With the help of the identities $\partial_{\bar{z}} \frac{1}{z} = \bar{\partial}_z \frac{1}{\bar{z}} = \pi \delta^{(2)}(z, \bar{z})$, one can verify these connections satisfy the sourced equations of motion. The connections are flat except for where the Wilson line sources them. We can obtain the specific form of the gauge field

$$A = L_0 \frac{dr}{r} + r L_1 dz + \sqrt{\frac{\mathcal{C}}{2}} \frac{1}{k} \left(\frac{dz}{z} - \frac{d\bar{z}}{\bar{z}} \right) (L_0 - r z L_1), \quad (\text{B.11})$$

$$\bar{A} = -L_0 \frac{dr}{r} - r L_{-1} d\bar{z} + \sqrt{\frac{\mathcal{C}}{2}} \frac{1}{k} \left(\frac{dz}{z} - \frac{d\bar{z}}{\bar{z}} \right) (L_0 - r \bar{z} L_{-1}). \quad (\text{B.12})$$

This solution produces the metric

$$ds^2 = \frac{dr^2}{r^2} + \frac{r^2 \left(-\sqrt{2} \sqrt{\mathcal{C}} k (z d\bar{z} - \bar{z} dz)^2 + \mathcal{C} (z d\bar{z} - \bar{z} dz)^2 - 2k^2 z \bar{z} dz d\bar{z} \right)}{2k^2 z \bar{z}}. \quad (\text{B.13})$$

Consider the map from plane to cylinder (τ, ϑ)

$$z = e^{\tau + i\vartheta}, \quad \bar{z} = e^{\tau - i\vartheta}, \quad (\text{B.14})$$

the metric becomes

$$ds^2 = \frac{dr^2}{r^2} - r^2 e^{2\tau} \left(d\tau^2 + \frac{d\vartheta^2 \left(\sqrt{2\mathcal{C}} - k \right)^2}{k^2} \right). \quad (\text{B.15})$$

One can see this is precisely the metric for AdS₃ with a conical singularity surrounding the Wilson line. The boundary geometry with Wilson line back-reaction becomes the n -sheet cylinder if we set the defect angle to be $2\pi(1 - \frac{1}{n})$. Then we can find the relation

$$\frac{\sqrt{2\mathcal{C}}}{k} = (n - 1) + O((n - 1)^2). \quad (\text{B.16})$$

Since the Wilson line action generates the n -sheet manifold, the partition function for n -sheet manifold can be written as

$$Z_n = \log W_{\mathcal{R}}(C) = -\sqrt{2\mathcal{C}}L(x_i, x_j), \quad (\text{B.17})$$

therefore the entanglement entropy can be obtained

$$S_{\text{EE}} = \lim_{n \rightarrow 1} \frac{1}{1-n} \log W_{\mathcal{R}}(C) = kL(x_i, x_j), \quad (\text{B.18})$$

which coincides with the RT formula.

The stress tensor corresponds to Poincaré AdS₃ vanishes, namely $\mathcal{L} = 0$ in (3.1). For the BTZ black hole, the stress tensor is a constant. According to the transformation law of the stress-tensor, we can transform the stress tensor to a constant by using a conformal map. After rescaling the radial coordinate, the BTZ black hole becomes Poincaré AdS₃ geometry with different period of the time direction. For the deformed BTZ black hole, we can perform the following coordinate transformation to (3.19)

$$w = (1 - \mu\mathcal{Q})\xi + \mathcal{Q}\bar{\xi}, \quad (\text{B.19})$$

$$\bar{w} = (1 - \mu\bar{\mathcal{Q}})\bar{\xi} + \bar{\mathcal{Q}}\xi, \quad (\text{B.20})$$

$$r = (1 - \mu\mathcal{Q})(1 - \mu\bar{\mathcal{Q}})\tilde{r}. \quad (\text{B.21})$$

so that the metric becomes the same as BTZ black hole

$$ds^2 = \frac{d\tilde{r}^2}{\tilde{r}^2} + \tilde{r}^2 \left(d\xi d\bar{\xi} + \frac{1}{\tilde{r}^2} (\mathcal{L}d\xi^2 + \bar{\mathcal{L}}d\bar{\xi}^2) + \frac{\mathcal{L}\bar{\mathcal{L}}}{\tilde{r}^4} d\xi d\bar{\xi} \right). \quad (\text{B.22})$$

One should note that the temperature (the period of Euclidean time) is different from the original BTZ black hole. The above consideration for the holographic entanglement entropy still holds for BTZ black hole and deformed BTZ black hole.

References

- [1] F. A. Smirnov and A. B. Zamolodchikov, “On space of integrable quantum field theories,” Nucl. Phys. B **915**, 363-383 (2017) [arXiv:1608.05499 [hep-th]].
- [2] A. Cavaglià, S. Negro, I. M. Szécsényi and R. Tateo, “ $T\bar{T}$ -deformed 2D Quantum Field Theories,” JHEP **10**, 112 (2016) [arXiv:1608.05534 [hep-th]].
- [3] L. McGough, M. Mezei and H. Verlinde, “Moving the CFT into the bulk with $T\bar{T}$,” JHEP **04**, 010 (2018) [arXiv:1611.03470 [hep-th]].
- [4] P. Kraus, J. Liu and D. Marolf, “Cutoff AdS₃ versus the $T\bar{T}$ deformation,” JHEP **07**, 027 (2018) [arXiv:1801.02714 [hep-th]].
- [5] A. B. Zamolodchikov, “Expectation value of composite field T anti-T in two-dimensional quantum field theory,” [arXiv:hep-th/0401146 [hep-th]].

- [6] J. Cardy, “The $T\bar{T}$ deformation of quantum field theory as random geometry,” JHEP **10**, 186 (2018) [arXiv:1801.06895 [hep-th]].
- [7] S. Dubovsky, V. Gorbenko and G. Hernández-Chifflet, “ $T\bar{T}$ partition function from topological gravity,” JHEP **09**, 158 (2018) [arXiv:1805.07386 [hep-th]].
- [8] S. Datta and Y. Jiang, “ $T\bar{T}$ deformed partition functions,” JHEP **08**, 106 (2018) [arXiv:1806.07426 [hep-th]].
- [9] O. Aharony, S. Datta, A. Giveon, Y. Jiang and D. Kutasov, “Modular invariance and uniqueness of $T\bar{T}$ deformed CFT,” JHEP **01**, 086 (2019) [arXiv:1808.02492 [hep-th]].
- [10] G. Bonelli, N. Doroud and M. Zhu, “ $T\bar{T}$ -deformations in closed form,” JHEP **06**, 149 (2018) [arXiv:1804.10967 [hep-th]].
- [11] G. Jorjadze and S. Theisen, “Canonical maps and integrability in $T\bar{T}$ deformed 2d CFTs,” [arXiv:2001.03563 [hep-th]].
- [12] S. Dubovsky, V. Gorbenko and M. Mirbabayi, “Asymptotic fragility, near AdS₂ holography and $T\bar{T}$,” JHEP **09**, 136 (2017) [arXiv:1706.06604 [hep-th]].
- [13] N. Callebaut, J. Kruthoff and H. Verlinde, “ $T\bar{T}$ deformed CFT as a non-critical string,” JHEP **04**, 084 (2020) [arXiv:1910.13578 [hep-th]].
- [14] A. J. Tolley, “ $T\bar{T}$ deformations, massive gravity and non-critical strings,” JHEP **06**, 050 (2020) [arXiv:1911.06142 [hep-th]].
- [15] M. Guica and R. Monten, “Infinite pseudo-conformal symmetries of classical $T\bar{T}$, $J\bar{T}$ and JT_a - deformed CFTs,” SciPost Phys. **11**, 078 (2021) [arXiv:2011.05445 [hep-th]].
- [16] M. Guica, “ $J\bar{T}$ -deformed CFTs as non-local CFTs,” [arXiv:2110.07614 [hep-th]].
- [17] W. Donnelly and V. Shyam, “Entanglement entropy and $T\bar{T}$ deformation,” Phys. Rev. Lett. **121**, no.13, 131602 (2018) [arXiv:1806.07444 [hep-th]].
- [18] S. Chakraborty, A. Giveon, N. Itzhaki and D. Kutasov, “Entanglement beyond AdS,” Nucl. Phys. B **935**, 290-309 (2018) [arXiv:1805.06286 [hep-th]].
- [19] J. Cardy, “ $T\bar{T}$ deformation of correlation functions,” JHEP **12**, 160 (2019) [arXiv:1907.03394 [hep-th]].
- [20] J. Kruthoff and O. Parrikar, “On the flow of states under $T\bar{T}$,” [arXiv:2006.03054 [hep-th]].
- [21] M. Guica, “On correlation functions in $J\bar{T}$ -deformed CFTs,” J. Phys. A **52**, no.18, 184003 (2019) [arXiv:1902.01434 [hep-th]].
- [22] B. Chen, L. Chen and P. X. Hao, “Entanglement entropy in $T\bar{T}$ -deformed CFT,” Phys. Rev. D **98**, no.8, 086025 (2018) [arXiv:1807.08293 [hep-th]].

- [23] S. He and H. Shu, “Correlation functions, entanglement and chaos in the $T\bar{T}/J\bar{T}$ -deformed CFTs,” JHEP **02**, 088 (2020) [arXiv:1907.12603 [hep-th]].
- [24] H. S. Jeong, K. Y. Kim and M. Nishida, “Entanglement and Rényi entropy of multiple intervals in $T\bar{T}$ -deformed CFT and holography,” Phys. Rev. D **100**, no.10, 106015 (2019) [arXiv:1906.03894 [hep-th]].
- [25] G. Jafari, A. Naseh and H. Zolfi, “Path Integral Optimization for $T\bar{T}$ Deformation,” Phys. Rev. D **101**, no.2, 026007 (2020) [arXiv:1909.02357 [hep-th]].
- [26] S. He, J. R. Sun and Y. Sun, “The correlation function of (1,1) and (2,2) supersymmetric theories with $T\bar{T}$ deformation,” JHEP **04**, 100 (2020) [arXiv:1912.11461 [hep-th]].
- [27] S. He and Y. Sun, “Correlation functions of CFTs on a torus with a $T\bar{T}$ deformation,” Phys. Rev. D **102**, no.2, 026023 (2020) [arXiv:2004.07486 [hep-th]].
- [28] S. Hirano, T. Nakajima and M. Shigemori, “ $T\bar{T}$ Deformation of stress-tensor correlators from random geometry,” JHEP **04**, 270 (2021) [arXiv:2012.03972 [hep-th]].
- [29] S. He, Y. Sun and Y. X. Zhang, “ $T\bar{T}$ -flow effects on torus partition functions,” JHEP **09**, 061 (2021) [arXiv:2011.02902 [hep-th]].
- [30] S. He, “Note on higher-point correlation functions of the $T\bar{T}$ or $J\bar{T}$ deformed CFTs,” Sci. China Phys. Mech. Astron. **64**, no.9, 291011 (2021) [arXiv:2012.06202 [hep-th]].
- [31] S. He and Y. Z. Li, “Higher Genus Correlation Functions in CFTs with $T\bar{T}$ Deformation,” [arXiv:2202.04810 [hep-th]].
- [32] Y. Jiang, “A pedagogical review on solvable irrelevant deformations of 2D quantum field theory,” Commun. Theor. Phys. **73**, no.5, 057201 (2021) [arXiv:1904.13376 [hep-th]].
- [33] G. Giribet, “ $T\bar{T}$ -deformations, AdS/CFT and correlation functions,” JHEP **02**, 114 (2018) [arXiv:1711.02716 [hep-th]].
- [34] W. Donnelly, E. LePage, Y. Y. Li, A. Pereira and V. Shyam, “Quantum corrections to finite radius holography and holographic entanglement entropy,” JHEP **05**, 006 (2020) [arXiv:1909.11402 [hep-th]].
- [35] A. Banerjee, A. Bhattacharyya and S. Chakraborty, “Entanglement Entropy for $T\bar{T}$ deformed CFT in general dimensions,” Nucl. Phys. B **948**, 114775 (2019) [arXiv:1904.00716 [hep-th]].
- [36] S. Griener, “Entanglement entropy and $T\bar{T}$ deformations beyond antipodal points from holography,” JHEP **11**, 171 (2019) [arXiv:1908.10372 [hep-th]].
- [37] P. Caputa, P. Caputa, S. Datta, S. Datta, Y. Jiang, Y. Jiang, P. Kraus and P. Kraus, “Geometrizing $T\bar{T}$,” JHEP **03**, 140 (2021) [erratum: JHEP **09**, 110 (2022)] [arXiv:2011.04664 [hep-th]].

- [38] E. A. Mazenc, V. Shyam and R. M. Soni, “A $T\bar{T}$ Deformation for Curved Spacetimes from 3d Gravity,” [arXiv:1912.09179 [hep-th]].
- [39] Y. Li and Y. Zhou, “Cutoff AdS₃ versus $T\bar{T}$ CFT₂ in the large central charge sector: correlators of energy-momentum tensor,” JHEP **12**, 168 (2020) [arXiv:2005.01693 [hep-th]].
- [40] S. Khoeini-Moghaddam, F. Omid and C. Paul, “Aspects of Hyperscaling Violating Geometries at Finite Cutoff,” JHEP **02**, 121 (2021) [arXiv:2011.00305 [hep-th]].
- [41] Y. Li, “Comments on large central charge $T\bar{T}$ deformed conformal field theory and cutoff AdS holography,” [arXiv:2012.14414 [hep-th]].
- [42] P. Kraus, R. Monten and R. M. Myers, “3D Gravity in a Box,” SciPost Phys. **11**, 070 (2021) [arXiv:2103.13398 [hep-th]].
- [43] M. Guica and R. Monten, “ $T\bar{T}$ and the mirage of a bulk cutoff,” SciPost Phys. **10**, no.2, 024 (2021) [arXiv:1906.11251 [hep-th]].
- [44] J. D. Brown and M. Henneaux, “Central Charges in the Canonical Realization of Asymptotic Symmetries: An Example from Three-Dimensional Gravity,” Commun. Math. Phys. **104**, 207-226 (1986)
- [45] R. Conti, S. Negro and R. Tateo, “The $T\bar{T}$ perturbation and its geometric interpretation,” JHEP **02**, 085 (2019) [arXiv:1809.09593 [hep-th]].
- [46] R. Conti, S. Negro and R. Tateo, “Conserved currents and $T\bar{T}_s$ irrelevant deformations of 2D integrable field theories,” JHEP **11**, 120 (2019) [arXiv:1904.09141 [hep-th]].
- [47] H. Ouyang and H. Shu, “ $T\bar{T}$ deformation of chiral bosons and Chern–Simons AdS₃ gravity,” Eur. Phys. J. C **80**, no.12, 1155 (2020) [arXiv:2006.10514 [hep-th]].
- [48] M. He and Y. h. Gao, “ $T\bar{T}/J\bar{T}$ -deformed WZW models from Chern-Simons AdS₃ gravity with mixed boundary conditions,” Phys. Rev. D **103**, no.12, 126019 (2021) [arXiv:2012.05726 [hep-th]].
- [49] S. Ebert, E. Hijano, P. Kraus, R. Monten and R. M. Myers, “Field Theory of Interacting Boundary Gravitons,” SciPost Phys. **13**, no.2, 038 (2022) [arXiv:2201.01780 [hep-th]].
- [50] P. Kraus, R. Monten and K. Roumpedakis, “Refining the cutoff 3d gravity/ $T\bar{T}$ correspondence,” JHEP **10**, 094 (2022) [arXiv:2206.00674 [hep-th]].
- [51] M. Asrat and J. Kudler-Flam, “ $T\bar{T}$, the entanglement wedge cross section, and the breakdown of the split property,” Phys. Rev. D **102**, no.4, 045009 (2020) [arXiv:2005.08972 [hep-th]].
- [52] K. Allameh, A. F. Astaneh and A. Hassanzadeh, “Aspects of holographic entanglement entropy for $T\bar{T}$ -deformed CFTs,” Phys. Lett. B **826**, 136914 (2022) [arXiv:2111.11338 [hep-th]].

- [53] M. R. Setare and S. N. Sajadi, “Holographic entanglement entropy in $T\bar{T}$ -deformed CFTs,” *Gen. Rel. Grav.* **54**, no.8, 85 (2022) [arXiv:2203.16445 [hep-th]].
- [54] S. He, Z. C. Liu and Y. Sun, “Entanglement entropy and modular Hamiltonian of free fermion with deformations on a torus,” *JHEP* **09**, 247 (2022) [arXiv:2207.06308 [hep-th]].
- [55] H. S. Jeong, W. B. Pan, Y. W. Sun and Y. T. Wang, “Holographic study of $T\bar{T}$ like deformed HV QFTs: holographic entanglement entropy,” [arXiv:2211.00518 [hep-th]].
- [56] E. Witten, “(2+1)-Dimensional Gravity as an Exactly Soluble System,” *Nucl. Phys. B* **311**, 46 (1988)
- [57] E. Lladrés, “General solutions in Chern-Simons gravity and $T\bar{T}$ -deformations,” *JHEP* **01**, 039 (2021) [arXiv:1912.13330 [hep-th]].
- [58] M. He, S. He and Y. h. Gao, “Surface charges in Chern-Simons gravity with $T\bar{T}$ deformation,” *JHEP* **03**, 044 (2022) [arXiv:2109.12885 [hep-th]].
- [59] S. Ebert, C. Ferko, H. Y. Sun and Z. Sun, “ $T\bar{T}$ in JT Gravity and BF Gauge Theory,” *SciPost Phys.* **13**, no.4, 096 (2022) [arXiv:2205.07817 [hep-th]].
- [60] M. Ammon, A. Castro and N. Iqbal, “Wilson Lines and Entanglement Entropy in Higher Spin Gravity,” *JHEP* **10**, 110 (2013) [arXiv:1306.4338 [hep-th]].
- [61] X. Huang, C. T. Ma and H. Shu, “Quantum correction of the Wilson line and entanglement entropy in the pure AdS₃ Einstein gravity theory,” *Phys. Lett. B* **806**, 135515 (2020) [arXiv:1911.03841 [hep-th]].
- [62] X. Huang, C. T. Ma, H. Shu and C. H. Wu, “U(1) CS theory vs SL(2) CS formulation: Boundary theory and Wilson line,” *Nucl. Phys. B* **984**, 115971 (2022) [arXiv:2011.03953 [hep-th]].
- [63] I. Bakhmatov, N. S. Deger, J. Gutowski, E. Ó. Colgáin and H. Yavartanoo, “Calibrated Entanglement Entropy,” *JHEP* **07**, 117 (2017) [arXiv:1705.08319 [hep-th]].
- [64] X. Huang and C. T. Ma, “Emergence of kinematic space from quantum modular geometric tensor,” *Phys. Lett. B* **825**, 136893 (2022) [arXiv:2110.08703 [hep-th]].
- [65] S. Ryu and T. Takayanagi, “Holographic derivation of entanglement entropy from AdS/CFT,” *Phys. Rev. Lett.* **96**, 181602 (2006) [arXiv:hep-th/0603001 [hep-th]].
- [66] S. Ryu and T. Takayanagi, “Aspects of Holographic Entanglement Entropy,” *JHEP* **08**, 045 (2006) [arXiv:hep-th/0605073 [hep-th]].
- [67] G. Dzhordzhadze, L. O’Raifeartaigh and I. Tsutsui, “Quantization of a relativistic particle on the SL(2,R) manifold based on Hamiltonian reduction,” *Phys. Lett. B* **336**, 388-394 (1994) [arXiv:hep-th/9407059 [hep-th]].

- [68] O. Aharony, S. S. Gubser, J. M. Maldacena, H. Ooguri and Y. Oz, “Large N field theories, string theory and gravity,” *Phys. Rept.* **323**, 183-386 (2000) [arXiv:hep-th/9905111 [hep-th]].
- [69] M. Banados, C. Teitelboim and J. Zanelli, “The Black hole in three-dimensional spacetime,” *Phys. Rev. Lett.* **69**, 1849-1851 (1992) [arXiv:hep-th/9204099 [hep-th]].
- [70] V. E. Hubeny, M. Rangamani and T. Takayanagi, “A Covariant holographic entanglement entropy proposal,” *JHEP* **07**, 062 (2007) [arXiv:0705.0016 [hep-th]].
- [71] M. Banados, “Three-dimensional quantum geometry and black holes,” *AIP Conf. Proc.* **484**, no.1, 147-169 (1999) [arXiv:hep-th/9901148 [hep-th]].
- [72] M. Rooman and P. Spindel, “Uniqueness of the asymptotic AdS(3) geometry,” *Class. Quant. Grav.* **18**, 2117-2124 (2001) [arXiv:gr-qc/0011005 [gr-qc]].
- [73] K. Krasnov, “On holomorphic factorization in asymptotically AdS 3-D gravity,” *Class. Quant. Grav.* **20**, 4015-4042 (2003) [arXiv:hep-th/0109198 [hep-th]].
- [74] A. Castro, D. M. Hofman and N. Iqbal, “Entanglement Entropy in Warped Conformal Field Theories,” *JHEP* **02**, 033 (2016) [arXiv:1511.00707 [hep-th]].
- [75] S. Chakrabarti and M. Raman, “Chiral Decoupling from Irrelevant Deformations,” *JHEP* **04**, 190 (2020) [arXiv:2001.06870 [hep-th]].
- [76] S. Chakrabarti, D. Gupta, A. Manna and M. Raman, “Irrelevant deformations of chiral bosons,” *JHEP* **02**, 028 (2021) [arXiv:2011.06352 [hep-th]].
- [77] D. D. Blanco, H. Casini, L. Y. Hung and R. C. Myers, “Relative Entropy and Holography,” *JHEP* **08**, 060 (2013) [arXiv:1305.3182 [hep-th]].
- [78] H. Casini and M. Huerta, “A c-theorem for the entanglement entropy,” *J. Phys. A* **40**, 7031-7036 (2007) [arXiv:cond-mat/0610375 [cond-mat]].
- [79] M. Asrat, “Entropic c -functions in $T\bar{T}$, $J\bar{T}$, $T\bar{J}$ deformations,” *Nucl. Phys. B* **960**, 115186 (2020) [arXiv:1911.04618 [hep-th]].
- [80] T. Hartman, “Entanglement Entropy at Large Central Charge,” [arXiv:1303.6955 [hep-th]].
- [81] M. Headrick, “Entanglement Renyi entropies in holographic theories,” *Phys. Rev. D* **82**, 126010 (2010) [arXiv:1006.0047 [hep-th]].
- [82] W. Fischler, A. Kundu and S. Kundu, “Holographic Mutual Information at Finite Temperature,” *Phys. Rev. D* **87**, no.12, 126012 (2013) [arXiv:1212.4764 [hep-th]].